PARALLEL DOMAIN DECOMPOSITION FORMULATION AND SOFTWARE FOR LARGE-SCALE SPARSE SYMMETRICAL/UNSYMMETRICAL AEROACOUSTIC APPLICATIONS

By:

D.T. NGUYEN

Final Report
For the Period January 15. 2001 – January 14, 2005

Prepared for
National Aeronautics and Space Administration
Langley Research Center
Hampton, Virginia 23681

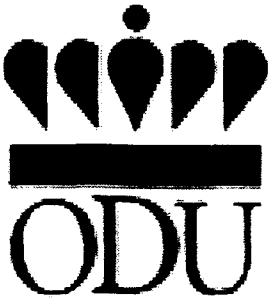

Technical Monitor and Collaborator
Dr. Willie R. Watson (NASA LaRC)

1. Introduction

The overall objectives of this research work are to formulate and validate efficient parallel algorithms, and to efficiently design/implement computer software for solving large-scale acoustic problems, arised from the unified frameworks of the finite element procedures.

The adopted parallel Finite Element (FE) Domain Decomposition (DD) procedures should fully take advantages of multiple processing capabilities offered by most modern high performance computing platforms for efficient parallel computation. To achieve this objective, the formulation needs to integrate efficient sparse (and dense) assembly techniques (see Section 2), hybrid (or mixed) direct and iterative equation solvers (see Section 3), proper pre_conditioned strategies, unrolling strategies [Ref. 6.5, Chapter 10], and effective processors' communicating schemes (see Section 3).

Finally, the numerical performance of the developed parallel finite element procedures will be evaluated by solving series of structural, and acoustic (symmetrical and un_symmetrical) problems (in different computing platforms). Comparisons with existing "commercialized" [Ref. 6.10] and/or "public domain" [Ref. 6.11] software are also included, whenever possible.

2. Algorithms and Application of Sparse Matrix Assembly and Equation Solvers for Aeroacoustics [Ref. 6.1]

(Please refer to the attached Journal Paper for this section)

Algorithms and Application of Sparse Matrix Assembly and Equation Solvers for Aeroacoustics

W. R. Watson*
NASA Langley Research Center, Hampton, Virginia 23681
D. T. Nguyen†
Old Dominion University, Norfolk, Virginia 23529
C. J. Reddy‡
EM, Inc., Hampton, Virginia 23666
V. N. Vatsa§
NASA Langley Research Center, Hampton, Virginia 23681
and
W. H. Tang¶
Hong Kong University of Science and Technology, Kowloon, Hong Kong, People's Republic of China

An algorithm for symmetric sparse equation solutions on an unstructured grid is described. Efficient, sequential sparse algorithms for degree-of-freedom reordering, supernodes, symbolic/numerical factorization, and forward/backward solution phases are reviewed. Three sparse algorithms for the generation and assembly of symmetric systems of matrix equations are presented. The accuracy and numerical performance of the sequential version of the sparse algorithms are evaluated over the frequency range of interest in a three-dimensional aeroacoustics application. Results show that the solver solutions are accurate using a discretization of 12 points per wavelength. Results also show that the first assembly algorithm is impractical for high-frequency noise calculations. The second and third assembly algorithms have nearly equal performance at low values of source frequencies, but at higher values of source frequencies the third algorithm saves CPU time and RAM. The CPU time and the RAM required by the second and third assembly algorithms are two orders of magnitude smaller than that required by the sparse equation solver. A sequential version of these sparse algorithms can, therefore, be conveniently incorporated into a substructuring (or domain decomposition) formulation to achieve parallel computation, where different substructures are handled by different parallel processors.

Nomenclature

$[A]$, $\{F\}$	=	global stiffness matrix and load vector without source effects
$[\bar{A}]$, $\{\bar{F}\}$	=	global stiffness matrix and loads vector with source effects
$[B]$, $[C]$, $[F]$	=	local element matrices for a rigid wall duct
$\{AN\}$, $\{a\}$	=	one-dimensional arrays containing sparse matrix coefficients
$[A^{(e)}]$, $\{F^{(e)}\}$	=	element stiffness matrix and loads vector
A_{IJ}, $A_{IJ}^{(e)}$, f_I	=	complex matrix coefficients
$[B]$, $[P]$	=	contributions to the element stiffness matrix due to the exit plane and interior elements
$[\mathcal{D}]$, $[\mathcal{L}]$	=	diagonal and unit lower triangular matrices
d_I	=	value of field variable at local node I
$[E]$	=	element degree-of-freedom matrix
$\{EN\}$	=	discrete error vector
E_i, N_m	=	error and three-dimensional basis functions
F	=	fill in resulting from matrix factorization
$\{F\}_I$	=	Ith component of $\{F\}$
$\{F(N)\}$	=	$\{F\}$ vector of length N
f, k	=	source frequency and free space wave number
H, L, W	=	height, length, and width of three-dimensional duct
$[HA]$, $\{ha\}$	=	matrix of pointers for sparse assembly
$[HA]_{IJ}$	=	coefficient of the Ith row and Jth column of $[HA]$
$[HA(N, M)]$	=	$[HA]$ an $N \times M$ matrix
h, l, w	=	height, length, and width of three-dimensional finite element
$\{IA\}$	=	array containing the number of nonzeroes per row
$\{IC\}$, $\{IE\}$, $\{IET\}$	=	arrays of starting locations of nonzero coefficients
$\{IP\}$, $\{IV\}$	=	permutation and inverse permutation vectors
$\{IR\}$, $\{JC\}$	=	array of row and column indexes for nonzero matrix coefficients
i	=	$\sqrt{-1}$
$\{JA\}$	=	array containing the column numbers of the nonzero off-diagonal matrix coefficients
$\{JE\}$	=	array of element connectivities
$\{JET\}$	=	array of element numbers connected to each degree of freedom

Received 16 February 2001; revision received 1 September 2001; accepted for publication 13 September 2001. Copyright © 2001 by the American Institute of Aeronautics and Astronautics, Inc. No copyright is asserted in the United States under Title 17, U.S. Code. The U.S. Government has a royalty-free license to exercise all rights under the copyright claimed herein for Governmental purposes. All other rights are reserved by the copyright owner. Copies of this paper may be made for personal or internal use, on condition that the copier pay the $10.00 per-copy fee to the Copyright Clearance Center, Inc., 222 Rosewood Drive, Danvers, MA 01923; include the code 0001-1452/02 $10.00 in correspondence with the CCC.

*Senior Research Scientist, Computational Modeling and Simulation Branch, Aerodynamics, Aerothermodynamics, and Acoustics Competency, Mail Stop 128; w.r.watson@larc.nasa.gov. Senior Member AIAA.

†Professor, Civil Engineering, and Head of Multidisciplinary Parallel-Vector Computation Center, 135 Kaufman Building; dnguyen@lions.odu.edu.

‡President and Chief Technical Officer, 24 Research Drive; cjreddy@emi-sys.com.

§Senior Research Scientist, Computational Modeling and Simulation Branch, Aerodynamics, Aerothermodynamics, and Acoustics Competency, Mail Stop 128; v.n.vatsa@larc.nasa.gov. Senior Member AIAA.

¶Professor and Chairperson, Civil and Structural Engineering Department.

M	=	number of nonzero coefficients in a sparse matrix, $N+NI$
ME	=	maximum number of elements connected to a degree of freedom
$\{MM\}$	=	array of element numbers connected to a degree of freedom
$\{MP\}$	=	array containing the number of elements connected to a degree of freedom
$\{MS\}$	=	master degree-of-freedom array
MZ	=	maximum number of nonzero coefficients per row
N	=	number of unknowns in the finite element discretization
NE, NP	=	number of finite elements and degrees of freedom per element
NF	=	number of fill ins during factorization of a matrix
NX, NY, NZ	=	total number of transverse, spanwise, and axial nodes
NI	=	number of nonzero, off-diagonal coefficients before factorization
$N2$	=	number of nonzero, off-diagonal coefficients after factorization
p	=	acoustic pressure field
p_m, p_s	=	acoustic pressure at local node m and source pressure
Relerr, u_0	=	relative error norm and uniform flow speed
S, V	=	surface and volume of a finite element
X	=	nonzero value that was modified during matrix factorization
x, y, z	=	Cartesian coordinates
x_I, y_J, z_K	=	transverse, spanwise, and axial locations of grid lines
β_{exit}	=	dimensionless exit admittance
$\partial p/\partial n$	=	derivative of the acoustic pressure normal to a surface
ζ, ζ_{exit}	=	dimensionless wall and exit impedance
$\{\Phi\}$	=	global vector of unknowns
$\{\Phi^e\}, \{\Phi^{I,J,K}\}$	=	local vectors of unknowns
$\{\Phi_{FF}\}, \{\Phi_{BB}\}$	=	intermediate vectors for forward and backward substitution
Φ_I, F_I^e	=	vector components
$\{\nabla\}, \nabla^2$	=	gradient vector and Laplace operator
$\bullet$	=	vector dot product

Subscripts

exit, s	=	exit and source plane index
F, R	=	factored and reordered matrix
FF, BB	=	forward and backward substitution
I, J	=	row and column index of a matrix

Superscripts

e	=	truss element number
I, J, K	=	grid line locator for three-dimensional duct
T	=	matrix or vector transpose
$*$	=	complex conjugate

I. Introduction

THREE-DIMENSIONAL aeroacoustics codes that can accurately predict the noise radiated from commercial aircraft are needed.[1] Currently, noise prediction codes require the use of a linear equation solver before radiated noise can be predicted. An optimizer must then run the noise predictive code on a digital computer hundreds of times to achieve an aircraft design with a minimal noise radiation signature.

Currently, industry and government aircraft noise predictive codes are either two-dimensional or treat only axisymmetric noise signatures.[1] When the volumes are three-dimensional, the currently used equation solvers require an excessive amount of CPU time and RAM for their assembly and solution. This excessive CPU time and computer storage restricts aircraft noise prediction codes to low-frequency sound sources in two-dimensional or axisymmetric environments.

Sparse equation solving technologies[2-14] have been developed and are well documented for several engineering applications, and the computational advantage of sparse solver technology over the more conventional technologies (such as band or skyline solvers) has been demonstrated. In addition, for practical engineering applications, system matrix equations must be developed for an unstructured grid to which boundary conditions are often difficult to apply. The finite element method is the simplest for generating the system matrix on an unstructured grid.

Only recently have sparse solver technologies been applied to aeroacoustics.[1,15] In Ref. 1, several direct and iterative equation solvers were evaluated to determine their applicability to two-dimensional duct aeroacoustics computations with the direct sparse solver emerging as the most promising. In Ref. 15, sparse solver equation solving methodology was extended to three-dimensional acoustically lined ducts. However, the work presented in Ref. 15 adopted the assembly strategy that is currently available in the literature for assembling system sparse matrix equations. This simple but inefficient assembly strategy precludes the use of sparse solvers for three-dimensional aeroacoustic computations.[15]

Most, if not all, major codes for analysis and optimal design allow users to select either iterative or direct equation solvers. For nacelle aeroacoustics computations, iterative solvers are not as robust as direct solvers because the nacelle equation system is poorly conditioned.[1] Iterative solution methods, when applied to systems of poorly conditioned equations, have the disadvantage that they do not converge, or they converge very slowly. A further disadvantage of applying iterative solution methods to solve the nacelle equation system is that the nacelle equation system often contains multiple right-hand sides. Iterative methods are not as efficient as direct methods on equation systems with multiple right-hand sides because the equation system must be reformed and resolved for each right-hand side.

The long-term objective of this research is to acquire the capability to design quiet aircraft in a fully three-dimensional aeroacoustic environment using direct sparse solver technologies and the finite element methodogy. The current paper has two objectives. The first objective is to bridge the gap between the aeroacousticians (who may not have a comprehensive knowledge of sparse assembly and equation solver technologies) and members of the sparse research community (who may not have comprehensive knowledge of finite element analysis and aeroacoustics). The second objective is to present efficient algorithms for assembling sparse matrix equations.

Section II describes three sparse assembly algorithms for generating systems of sparse linear equations. Section III describes the template that is used to develop a complete, unstructured grid, finite element code, that is, equation reordering, symbolic/numerical factorization, supernodes/loop unrolling, and forward/backward solution phases. Section IV presents a detailed formulation of the element stiffness matrices that will be assembled using the sparse assembly algorithms to form the system matrix for a three-dimensional duct aeroacoustics application. Finally, Sec. V discusses the accuracy and numerical performance of the developed algorithms over the frequency range of interest for a three-dimensional aeroacoustics application. Note that although the sparse algorithms presented assume that the system matix equation is symmetric, these algorithms are easily extendible to nonsymmetric systems of equations. The algorithms can also be conveniently incorporated into a substructuring (or domain decomposition) formulation to take advantage parallel computation to further reduce CPU time and RAM.

II. Sparse Assembly Algorithms for Symmetric Systems

Figure 1 is a two-dimensional truss (or rod) structure assembled from individual truss elements labeled (1), (2), . . . , (13) that are interconnected at eight nodes labeled 1, 2, . . . , 8. An element (e) of the structure is assumed to possess only two points of connection, and the external loads are assumed to be applied at the nodes of the truss elements. Only a single degree of freedom (DOF) at each node is assumed. To further simplify discussions, it is assumed that, by a separate calculation, the element stiffness matrix and external load vector for the truss element (e) are known and expressed as

$$\begin{bmatrix} A_{21}^{(e)} & A_{22}^{(e)} \end{bmatrix} \qquad \begin{bmatrix} F_2^{(e)} \end{bmatrix}$$

Under the assumption of Eq. (1), the 13 truss elements (Fig. 1) may be assembled using the rules of finite element assembly[16] to obtain the system matrix equation

$$[A]\{\Phi\} = \{F\} \tag{2}$$

$$[A(N,N)] = \sum_{e=1}^{e=13} \left[A^{(e)}(2,2)\right]$$

$$= \begin{bmatrix} A_{11} & A_{12}^{(4)} & 0 & A_{21}^{(3)} & A_{21}^{(5)} & 0 & A_{21}^{(1)} & 0 \\ A_{21}^{(4)} & A_{22} & A_{12}^{(7)} & 0 & A_{21}^{(8)} & 0 & 0 & 0 \\ 0 & A_{21}^{(7)} & A_{33} & 0 & A_{21}^{(9)} & A_{21}^{(11)} & 0 & A_{21}^{(12)} \\ A_{12}^{(3)} & 0 & 0 & A_{44} & A_{12}^{(6)} & 0 & A_{21}^{(2)} & 0 \\ A_{21}^{(5)} & A_{12}^{(8)} & A_{12}^{(9)} & A_{21}^{(6)} & A_{55} & A_{12}^{(10)} & 0 & 0 \\ 0 & 0 & A_{12}^{(11)} & 0 & A_{21}^{(10)} & A_{66} & 0 & A_{12}^{(13)} \\ A_{12}^{(1)} & 0 & 0 & A_{12}^{(2)} & 0 & 0 & A_{77} & 0 \\ 0 & 0 & A_{12}^{(12)} & 0 & 0 & A_{21}^{(13)} & 0 & A_{88} \end{bmatrix} \tag{3}$$

$$A_{11} = A_{22}^{(1)} + A_{22}^{(3)} + A_{11}^{(4)} + A_{22}^{(5)}, \qquad A_{22} = A_{22}^{(4)} + A_{11}^{(7)} + A_{22}^{(8)}$$

$$A_{33} = A_{22}^{(7)} + A_{22}^{(9)} + A_{22}^{(11)} + A_{22}^{(12)}, \qquad A_{44} = A_{22}^{(3)} + A_{11}^{(3)} + A_{11}^{(6)}$$

$$A_{55} = A_{22}^{(5)} + A_{22}^{(6)} + A_{11}^{(8)} + A_{11}^{(9)} + A_{11}^{(10)}$$

$$A_{66} = A_{22}^{(6)} + A_{11}^{(11)} + A_{11}^{(13)}, \qquad A_{77} = A_{11}^{(1)} + A_{11}^{(2)}$$

$$A_{88} = A_{22}^{(12)} + A_{22}^{(13)} \tag{4}$$

$$\{\Phi(N)\} = \begin{Bmatrix} \Phi_1 \\ \Phi_2 \\ \Phi_3 \\ \Phi_4 \\ \Phi_5 \\ \Phi_6 \\ \Phi_7 \\ \Phi_8 \end{Bmatrix}$$

$$\{F(N)\} = \begin{Bmatrix} F_2^{(1)} + F_2^{(3)} - F_1^{(4)} + F_2^{(5)} \\ F_2^{(4)} - F_1^{(7)} + F_2^{(8)} \\ F_2^{(7)} - F_2^{(9)} - F_2^{(11)} + F_1^{(12)} \\ F_2^{(3)} - F_1^{(3)} - F_1^{(6)} \\ F_2^{(5)} + F_2^{(6)} - F_2^{(8)} + F_1^{(9)} - F_1^{(10)} \\ F_2^{(6)} - F_1^{(11)} + F_1^{(13)} \\ F_1^{(1)} - F_2^{(3)} - F_1^{(2)} \\ F_2^{(12)} - F_2^{(13)} \end{Bmatrix} \tag{5}$$

Although only a single DOF (Φ_I) is assumed at node I, the discussion to follow is easily extended to q DOF per node by extending the coefficients in $[A]$, that is, $A_{IJ}^{(e)}$, to $q \times q$ submatrices. The rules of matrix algebra would then be applied to each $q \times q$ submatrix as if it were a scalar.

A. Sparse Data Formats for the System Matrix

For the sake of brevity, in the discussions to follow it will be assumed that the element stiffness matrix is symmetric so that

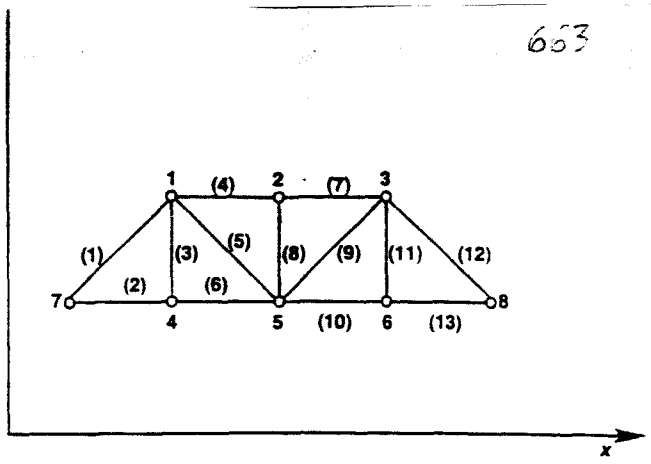

Fig. 1 Two-dimensional truss sample problem.

$$\left[A^{(e)}\right]_{JI} = \left[A^{(e)}\right]_{IJ} \tag{6}$$

Under the assumptions of Eq. (6), the system matrix $[A]$ is also symmetric and can be written in the form

$$[A(N,N)]$$

$$= \begin{bmatrix} A_{11} & A_{12}^{(4)} & 0 & A_{12}^{(3)} & A_{12}^{(5)} & 0 & A_{12}^{(1)} & 0 \\ A_{12}^{(4)} & A_{22} & A_{12}^{(7)} & 0 & A_{12}^{(8)} & 0 & 0 & 0 \\ 0 & A_{12}^{(7)} & A_{33} & 0 & A_{12}^{(9)} & A_{12}^{(11)} & 0 & A_{12}^{(12)} \\ A_{12}^{(3)} & 0 & 0 & A_{44} & A_{12}^{(6)} & 0 & A_{12}^{(2)} & 0 \\ A_{12}^{(5)} & A_{12}^{(8)} & A_{12}^{(9)} & A_{12}^{(6)} & A_{55} & A_{12}^{(10)} & 0 & 0 \\ 0 & 0 & A_{12}^{(11)} & 0 & A_{12}^{(10)} & A_{66} & 0 & A_{12}^{(13)} \\ A_{12}^{(1)} & 0 & 0 & A_{12}^{(2)} & 0 & 0 & A_{77} & 0 \\ 0 & 0 & A_{12}^{(12)} & 0 & 0 & A_{12}^{(13)} & 0 & A_{88} \end{bmatrix} \tag{7}$$

The sparse descriptions of any symmetric system matrix $[A]$ [see Eq. (7)] is fully described by the four one-dimensional vectors

$$\{IA(N+1)\} = \{4, 2, 3, 2, 1, 1, 0, 0\}^T$$

$$\{JA(NA)\} = \{2, 4, 5, 7, 3, 5, 5, 6, 8, 5, 7, 6, 8\}^T \tag{8}$$

$$\{AD(N)\} = \{A_{11}, A_{22}, A_{33}, A_{44}, A_{55}, A_{66}, A_{77}, A_{88}\}^T \tag{9}$$

$$\{AN(NA)\} = \left\{A_{12}^{(4)}, A_{12}^{(3)}, A_{12}^{(5)}, A_{12}^{(1)}, A_{12}^{(7)}, A_{12}^{(8)}, A_{12}^{(9)}, A_{12}^{(11)}, A_{12}^{(12)}, A_{12}^{(6)}, A_{12}^{(2)}, A_{12}^{(10)}, A_{12}^{(13)}\right\}^T \tag{10}$$

B. Application of Boundary Conditions

In most engineering applications, the field variable at several boundary nodes may require constraints to satisfy a Dirichlet boundary condition of the form

$$\{\Phi\}_I = d_I \tag{11}$$

where d_I is the specified value of the field variable at node I. Dirichlet boundary conditions may be applied at the element or system level. The impact of applying Dirichlet boundary conditions on the system matrix equation is identical whether applied at the element or system level. We will show the relatively easy process of applying Dirichlet boundary conditions at the element level and their impact on the system matrix equation [Eq. (2)].

The process for inserting the Dirichlet boundary condition, $\{\Phi\}_I = d_I$, is as follows:

1) The column of $[A^{(e)}]$ corresponding to the Ith DOF is multiplied by d_I, and the result is subtracted from $\{F^{(e)}\}$.

2) The column corresponding to the Ith DOF in $[A^{(e)}]$ is made zero.

3) The row corresponding to the Ith DOF in $[A^{(e)}]$ is made zero.

4) The modified element matrix and the modified element load vector are assembled.

5) $[A]_{II}$ is made equal to unity, and $\{F\}_I$ is made equal to d_I.

Thus, applying Dirichlet boundary conditions to the system matrix equation modifies Eq. (2) to

$$[\bar{A}]\{\Phi\} = \{\bar{F}\} \tag{12}$$

The numerical values of the coefficients in the modified system matrix $[\bar{A}]$ remain unchanged from those in $[A]$, except for a few that are made zero during the application of the Dirichlet boundary conditions. Therefore, we will illustrate application of the assembly algorithms to the nonzero pattern of $[A]$.

C. Sparse Assembly Algorithms

Three symmetric sparse assembly algorithms will be explained in this section. The purpose of each assembly algorithm is to generate the system loads vector $\{\bar{F}\}$ and the four vectors derived by Eqs. (8–10), which correspond to $[\bar{A}]$. The assembly algorithms are discussed starting with the simplest and proceeding to the most complex.

1. *Algorithm 1*

The main ideas of this algorithm can be summarized by the following computational tasks:

1) Find how many and which elements are connected to each DOF.

a) Input data for N, NE, NP, and the elements connectivity (see Fig. 1).

b) Compute the number of elements associated with each DOF, and store this information into the one-dimensional integer vector $\{MP(N)\}$.

c) Find the element numbers associated with each DOF, and store this information into the two-dimensional integer matrix $[MM(N, ME)]$.

2) Retrieve the stiffness matrix attached to each DOF, perform sparse matrix assembly one row at a time, and extract the four one-dimensional vectors required for the sparse equation solver.

2. *Algorithm 2*

The nonzero patterns of the symmetrical matrix $[A]$ [see Eq. (7)] for the two-dimensional truss example problem (Fig. 1) can be completely described by the two one-dimensional integer vectors

$$\{IR(M)\} = \{7, 1, 1, 4, 4, 1, 1, 2, 1, 5, 4, 2, 3, 2, 3, 5, 6, 3, 3, 8, 6\}^T \tag{13}$$

$$\{JC(M)\} = \{7, 7, 1, 7, 4, 4, 2, 2, 5, 5, 5, 3, 3, 5, 5, 6, 6, 6, 8, 8, 8\}^T \tag{14}$$

and the following integer matrix:

$$[HA(N, MZ)] = \begin{bmatrix} 2 & 3 & 6 & 7 & 9 \\ 8 & 12 & 14 & 0 & 0 \\ 13 & 15 & 18 & 19 & 0 \\ 4 & 5 & 11 & 0 & 0 \\ 10 & 16 & 0 & 0 & 0 \\ 17 & 21 & 0 & 0 & 0 \\ 1 & 0 & 0 & 0 & 0 \\ 20 & 0 & 0 & 0 & 0 \end{bmatrix} \tag{15}$$

The two one-dimensional integer vectors in Eqs. (13) and (14) are constructed by cycling through each element (e) in increasing order and then determining the row and column index of each nonzero coefficient from the connectivity array for each element (Fig. 1). Note that the matrix $[HA]$ contains locations (or pointers) that are used to refer to vectors $\{IR\}$ and $\{JC\}$. For example, the values of $[HA]_{41} = 4$, $[HA]_{42} = 5$, and $[HA]_{43} = 11$ indicate that row 4 of matrix $[A]$ will have these nonzero terms. The exact locations (row and column numbers) of those three nonzero terms in $[A]$ can be referred to as

$$\{IR\}_4 = 4, \qquad \{JC\}_4 = 7, \qquad \{IR\}_5 = 4$$

$$\{JC\}_5 = 4, \qquad \{IR\}_{11} = 4, \qquad \{JC\}_{11} = 5 \tag{16}$$

Thus, the three nonzero terms of the fourth row of $[A]$ are located at row 4, column 7; row 4, column 4; and row 4, column 5, respectively [see Eq. (7)].

The integer matrix $[HA]$ and system matrix $[A]$ can be alternatively stored as one-dimensional vectors:

$$\{ha(M)\} = \{2, 3, 6, 7, 9, 8, 12, 14, 13, 15, 18, 19,$$

$$4, 5, 11, 10, 16, 17, 21, 1, 20\}^T \tag{17}$$

$$\{a(M)\} = \left\{A_{12}^{(4)}, A_{12}^{(3)}, A_{22}, A_{12}^{(7)}, A_{33}, A_{12}^{(8)}, A_{12}^{(12)}, A_{12}^{(6)}, A_{44}, A_{12}^{(2)}, A_{66}, A_{12}^{(13)}, A_{12}^{(5)}, A_{12}^{(1)}, A_{12}^{(11)}, A_{12}^{(9)}, A_{55}, A_{12}^{(10)}, A_{88}, A_{11}, A_{77}\right\}^T \tag{18}$$

The main ideas of algorithm 2 can be summarized by the following computational tasks:

1) After initializing $\{ha\}$ to a zero vector, process all elements (in ascending order) to obtain the integer vectors $\{IR\}$ and $\{JC\}$ while assembling $[A]$ into $\{a\}$.

2) Separate the diagonal and nonzero off-diagonal terms of $[A]$ from $\{a\}$ and store this information in $\{AD\}$ and $\{AN\}$. Separate the diagonal and off-diagonal terms in $\{IR\}$ and $\{JC\}$, and compute $\{JA\}$ and $\{IA\}$.

3. *Algorithm 3*

The nonzero patterns of the symmetrical system matrix $[A]$ can be completely described by $\{JA\}$ and the following one-dimensional integer vector:

$$\{IC(N+1)\} = \{1, 5, 7, 10, 12, 13, 14, 14, 14\}^T \tag{19}$$

where

$$\{JA\}_I = \{IC\}_{I+1} - \{IC\}_I \tag{20}$$

and the variable NJ can be conveniently computed as

$$NJ = \{IC\}_{N+1} - \{IC\}_1 \tag{21}$$

The element connectivity information for the two-dimensional truss sample problem (Fig. 1) is fully described by the element-DOF matrix

$$[E(NE, NJ)] = \begin{bmatrix} 1 & 0 & 0 & 0 & 0 & 0 & 1 & 0 \\ 0 & 0 & 0 & 1 & 0 & 0 & 1 & 0 \\ 1 & 0 & 0 & 1 & 0 & 0 & 0 & 0 \\ 1 & 1 & 0 & 0 & 0 & 0 & 0 & 0 \\ 1 & 0 & 0 & 0 & 1 & 0 & 0 & 0 \\ 0 & 0 & 0 & 1 & 1 & 0 & 0 & 0 \\ 0 & 1 & 1 & 0 & 0 & 0 & 0 & 0 \\ 0 & 1 & 0 & 0 & 1 & 0 & 0 & 0 \\ 0 & 0 & 1 & 0 & 1 & 0 & 0 & 0 \\ 0 & 0 & 0 & 0 & 1 & 1 & 0 & 0 \\ 0 & 0 & 1 & 0 & 0 & 1 & 0 & 0 \\ 0 & 0 & 1 & 0 & 0 & 0 & 0 & 1 \\ 0 & 0 & 0 & 0 & 0 & 1 & 0 & 1 \end{bmatrix} \tag{22}$$

Each row of $[E]$ contains exactly two nonzeros because each element has two points of connection, or nodes, to the structure. Thus, $[E]_{IJ}$ is nonzero only if node J is a node for element I. For example, the first row of $[E]$ contains a unit value only in columns 1 and 7, indicating that the first element of the truss is connected to nodes 1 and 7 only

(Fig. 1). The concept of an element-DOF matrix is easily extended to q DOF per node by extending each of the unity coefficients in $[E]$ to a $q \times q$ identity matrix.

To minimize the RAM, it is convenient to describe the element-DOF matrix $[E]$ by the two one-dimensional vectors

$$\{IE(NE+1)\} = \{1, 3, 5, 7, 9, 11, 13, 15, 17, 19, 21, 23, 25, 27\}^T \tag{23}$$

$$\{JE(NE \times NP)\} = \{7, 1, 7, 4, 4, 1, 1, 2, 1, 5,$$
$$4, 5, 2, 3, 5, 2, 5, 3, 5, 6, 6, 3, 3, 8, 6, 8\}^T \tag{24}$$

and the transpose of the element-DOF matrix ($[E]^T$) by the following two one-dimensional vectors:

$$\{IET(N+1)\} = \{1, 5, 8, 12, 15, 20, 23, 25, 27\}^T \tag{25}$$

$$\{JET(NE \times NP)\} = \{1, 3, 4, 5, 4, 7, 8, 7, 9, 11, 12, 2, 3,$$
$$6, 5, 6, 8, 9, 10, 10, 11, 13, 1, 2, 12, 13\}^T \tag{26}$$

The main ideas of algorithm 3 can be summarized by the following computational tasks:

1) Assume that $\{IE\}$, $\{JE\}$, $\{IET\}$, and $\{JET\}$ have already been defined from the connectivity information (see Fig. 1).

a) Compute $\{IC\}$ and $\{JA\}$ (symbolic assembly phase).

b) Compute $\{IA\}$ from Eq. (20).

2) Assume that vectors $\{IA\}$ and $\{JA\}$ have already been defined from the symbolic assembly (task 1). Compute $\{AN\}$ and $\{AD\}$ from $[A^{(e)}]$ (numerical assembly phase).

III. Sparse Algorithms for Solving Symmetrical Equations

In this section, the major tasks involved in solving sparse systems of linear equations are briefly explained. The success of the sparse solver is due to improved technologies (i.e., equation reordering, matrix decomposition, supernodes and loop unrolling, forward/backward solution phases) and bookkeeping strategies ideal for implementation on a digital computer. More detailed information on improved technologies can be obtained from Refs. 2–14.

A. Sparse Reordering Algorithms

After imposing the boundary conditions, the modified stiffness matrix $[\bar{A}]$ can be obtained from $[A]$ as indicated in the discussions before Eq. (12). Equation (12) should never be solved directly. To further simplify the discussions, we will assume that matrix $[\bar{A}]$ has the following numerical values:

$$[\bar{A}(N, N)] = \begin{bmatrix} 110 & 7 & 4 & 0 & 5 & 3 \\ 7 & 112 & 0 & 2 & 0 & 0 \\ 4 & 0 & 66 & 0 & 0 & 0 \\ 0 & 2 & 0 & 11 & 1 & 0 \\ 5 & 0 & 0 & 1 & 88 & 0 \\ 3 & 0 & 0 & 0 & 0 & 44 \end{bmatrix} \tag{27}$$

Thus, in this case $N = 6$ and $N1 = 6$. During the factorization phase, many of the zero-value terms appearing in Eq. (27) may become nonzero. For maximum efficiency of storage and solution time, the equations are reordered so that the number of nonzero terms that occur during factorization are minimized. These extra nonzero terms created during the factorization of $[\bar{A}]$ are referred to as fill ins and are denoted by the symbols F in the following equation:

$$[\bar{A}_F(N, N)] = \begin{bmatrix} X & X & X & 0 & X & X \\ & X & F & X & F & F \\ & & X & F & F & F \\ & & & X & X & F \\ & & & & X & F \\ & & & & & X \end{bmatrix} \tag{28}$$

In Eq. (28), one has eight extra (or new) nonzero fill ins. As a result,

$$NF = 8 \tag{29}$$

$$N2 = N1 + NF = 6 + 8 = 14 \tag{30}$$

In general, the number of nonzero coefficients in the upper triangular part of $[\bar{A}]$ after factorization ($N2$) is much larger than those before factorization ($N1$).

The purpose of reordering algorithms [multiple minimum degrees (MMD), nested dissection, or METIS algorithms] is to rearrange the nonzero terms of $[\bar{A}]$, defined in Eq. (27), to different locations so that $N2$ is minimized.[5,17–23] For example, applying the MMD reordering algorithm to $[\bar{A}]$ will result in the following permutation and inverse permutation vectors:

$$\{IP(N)\} = \{5, 6, 3, 1, 4, 2\}^T, \qquad \{IV(N)\} = \{4, 6, 3, 5, 1, 2\}^T \tag{31}$$

With the permutation array $\{IP\}$, the matrix $[\bar{A}]$ in Eq. (27) can be transformed into

$$[\bar{A}_R(N, N)] = \begin{bmatrix} 11 & 0 & 0 & 1 & 0 & 2 \\ 0 & 44 & 0 & 0 & 3 & 0 \\ 0 & 0 & 66 & 0 & 4 & 0 \\ 1 & 0 & 0 & 88 & 5 & 0 \\ 0 & 3 & 4 & 5 & 110 & 7 \\ 2 & 0 & 0 & 0 & 7 & 112 \end{bmatrix} \tag{32}$$

Now, if one factorizes $[\bar{A}_R]$, there will be only one fill in that occurs, as follows:

$$[\bar{A}_{RF}(N, N)] = \begin{bmatrix} X & 0 & 0 & X & 0 & X \\ & X & 0 & 0 & X & 0 \\ & & X & 0 & X & 0 \\ & & & X & X & F \\ & & & & X & X \\ & & & & & X \end{bmatrix} \tag{33}$$

B. Sparse Symbolic Factorization

The reordered matrix $[\bar{A}_R]$ can be described by the following four one-dimensional vectors:

$$\{IA(N+1)\} = \{1, 3, 4, 5, 6, 7, 7\}^T$$

$$\{JA(N1)\} = \{4, 6, 5, 5, 5, 6\}^T \tag{34}$$

$$\{AD(N)\} = \{11, 44, 66, 88, 110, 112\}^T$$

$$\{AN(N1)\} = \{1, 2, 3, 4, 5, 7\}^T \tag{35}$$

In this example, $N = 6$ and $N1 = 6$. Before performing the numerical factorization, it is necessary to go through the sparse symbolic factorization, so that the following hold true:

1) The nonzero pattern of $[\bar{A}_{RF}]$ can be determined (including the locations of fill ins).

2) The value of $N2$ can be determined so that adequate computer memory can be allocated for the subsequent sparse numerical factorization phase.

On completion of the sparse symbolic factorization phase, the nonzero patterns of $[\bar{A}_{RF}]$ are completely known, and the modified versions of Eqs. (34) and (35) for the factored matrix $[\bar{A}_{RF}]$ can be computed as

$$\{IA(N+1)\} = \{1, 3, 4, 5, 7, 8, 8\}^T$$

$$\{JA(N2)\} = \{4, 6, 5, 5, 5, 6, 6\}^T \tag{36}$$

In this case,

$$N2 = N1 - NF = 6 + 1 = 7 \tag{37}$$

Efficient sparse symbolic factorization algorithms and detailed FORTRAN coding can be found elsewhere.[5,5–7]

C. Finding Supernodes

To understand the concept of a supernode (or master node), notice that, in Eq. (33), rows 2–3 and 4–5 have the same nonzero patterns. That is, the nonzero terms in rows 2–3 correspond to the same column numbers. Equation (33) can be used to define a master DOF vector

$$\{MS(N)\} = \{1, 2, 0, 2, 0, 1\}^T \tag{38}$$

The master DOF vector $\{MS\}$ is based on the assumed system matrix $[\bar{A}_{RF}]$ defined in Eq. (33). Once Eq. (38) has been defined, effective loop-unrolling techniques[2,23] can be used to improve computational speed during the sparse numerical factorization phase.

D. Sparse Numerical Factorization Phase

The strategies employed in this phase are quite similar to the ones used during the sparse symbolic factorization phase and have been well documented in the literature.[5,24] The reordered system matrix $[\bar{A}_R]$ can be decomposed or factorized as

$$[\bar{A}_R] = [\mathcal{L}][\mathcal{D}][\mathcal{L}]^T \tag{39}$$

Here, $[\mathcal{D}]$ is a diagonal and $[\mathcal{L}]$ is unit lower triangular matrix, and

$$[\mathcal{D}]_{II} = \begin{Bmatrix} [\bar{A}_R]_{11} & (I = 1) \\ [\bar{A}_R]_{II} - \sum_{K=1}^{I-1} [\mathcal{D}]_{KK}[\mathcal{L}]_{KI} & (I = 2, 3, \ldots, N) \end{Bmatrix} \tag{40}$$

$$[\mathcal{L}]_{IJ} = \begin{Bmatrix} \dfrac{[\bar{A}_R]_{IJ}}{[\mathcal{D}]_{II}} & (I = 1, \quad J = 2, \ldots, N) \\ [\bar{A}_R]_{IJ} - \sum_{K=1}^{I-1} \dfrac{[\mathcal{D}]_{KK}[\mathcal{L}]_{KI}[\mathcal{L}]_{KJ}}{[\mathcal{D}]_{II}} & (I = 1, \quad J = I+1, \ldots, N) \end{Bmatrix} \tag{41}$$

E. Solution to the System Matrix Equation

The solution to the system matrix equation [Eq. (12)] is obtained in three phases:

1) In the first phase (forward solution phase), an intermediate solution vector $\{\Phi_{FF}\}$ is computed from the solution of the matrix equation

$$[\mathcal{L}]\{\Phi_{FF}\} = \{\bar{F}_R\} \tag{42}$$

2) In the second phase (backward solution phase), a vector $\{\Phi_{BB}\}$ is computed from the matrix equation

$$[\mathcal{D}][\mathcal{L}]^T\{\Phi_{BB}\} = \{\Phi_{FF}\} \tag{43}$$

3) In the third phase (back transformation phase), the vector $\{\Phi_{BB}\}$ is transformed back to the original unknown vector $\{\Phi\}$ by utilizing the inverse permutation vector $\{IV\}$.

IV. Three-Dimensional Aeroacoustics Application

The developed algorithm will be exercised to study the propagation of acoustic pressure waves in a three-dimensional duct lined with sound absorbing materials (acoustic liners) as depicted in Fig. 2. The duct is spanned by axial coordinate z, transverse coordinate x, and spanwise coordinate y. The source plane is located at $z = 0$, and the source plane acoustic pressure p_s is assumed known. At the exit plane, the dimensionless exit acoustic impedance ζ_{exit} is assumed known. In the duct, air is flowing along the positive z axis at a subsonic speed of u_0, and the duct has acoustic liners along its upper, lower, and two sidewalls. The duct walls are assumed to be locally reacting so that the sound absorbing properties of the acoustic liners results from the dimensionless wall impedance ζ that is assumed known. The sound source pressure, dimensionless exit impedance, and dimensionless wall impedance are assumed functions of position along their respective boundaries.

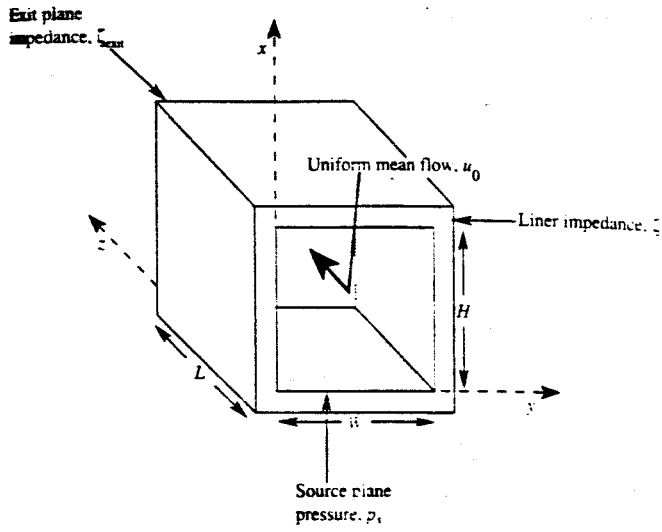

Fig. 2 Three-dimensional duct and coordinate system.

A. Mathematical Formulation

The mathematical formulation of the duct acoustics problem (Fig. 2) does not lead to a boundary value problem that is formally self-adjoint and will not lead to a symmetric system matrix when airflow is considered. Thus, the analysis in the foregoing discussion does not allow for airflow because the current paper focuses on symmetric systems. With zero airflow in the duct ($u_0 = 0$), the mathematical problem is to find the solution to Helmholtz's equation[15]

$$\nabla^2 p + k^2 p = 0 \tag{44}$$

Along the source plane of the duct ($z = 0$), the boundary condition is given in term of a Dirichlet boundary condition:

$$p = p_s \tag{45}$$

The wall boundary condition is

$$\frac{\partial p}{\partial n} = -ik\frac{p}{\zeta} \tag{46}$$

At the duct termination ($z = L$), the ratio of acoustic pressure to the axial component of acoustic particle velocity is proportional to the known dimensionless exit impedance. When expressed in terms of the acoustic pressure, this boundary condition is

$$\frac{\partial p}{\partial n} = -ik\frac{p}{\zeta_{exit}} \tag{47}$$

Equations (44–47) form a well-posed boundary value problem for which exact solutions for the acoustic pressure field are generally not known. A solution for the acoustic pressure field satisfying this boundary value problem is required to predict and reduce the radiated noise. An approximate solution for the acoustic pressure field can be obtained using numerical techniques such as the finite element method.

B. Finite Element Model

The approximate solution for the sound field in the duct is obtained by subdividing the duct and representing the acoustic field within each subdivision by relatively simple functions. Because the duct of interest is a rectangular prism, the computational domain is divided into a number of smaller rectangular prisms (or elements) as shown in Fig. 3. These elements are considered interconnected at joints called nodes. The most widely used method for locating the nodes in the discretization is to divide the physical volume into NX, NY, and NZ grid lines in the x, y, and z directions, respectively, as shown in Fig. 3. Each node of an element can be located by identifying an ordered triplet, (x_I, y_J, z_K). Similarly, each element in the assemblage can be identified by an ordered triplet of integers (I, J, K). A typical rectangular prism element (I, J, K) is shown in Fig. 4. Each element consists of eight local node numbers labeled

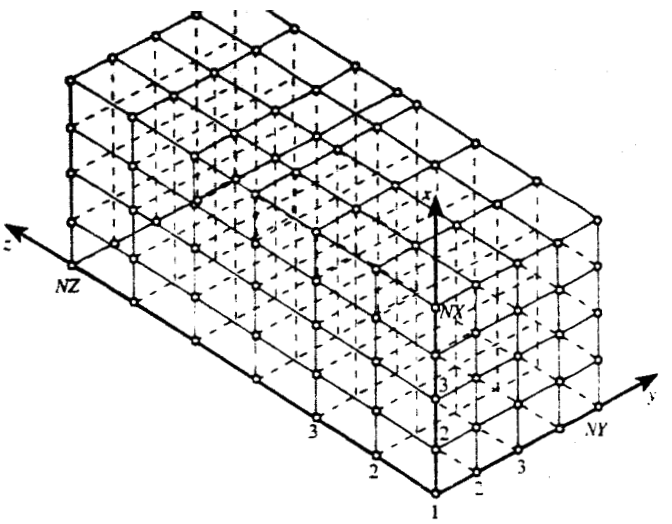

Fig. 3 Three-dimensional finite element discretization.

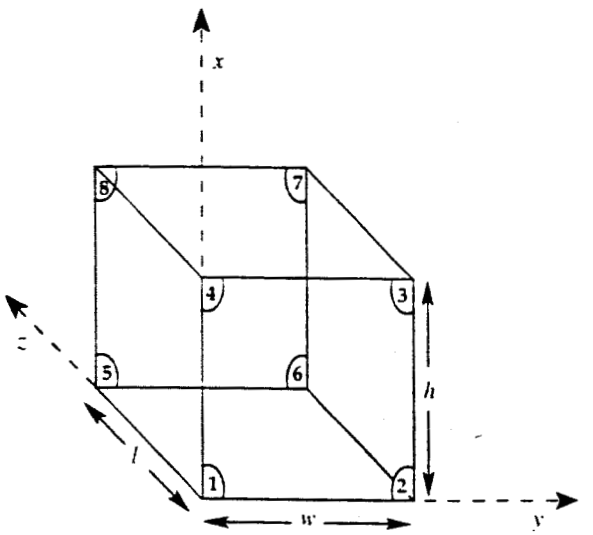

Fig. 4 Typical three-dimensional element and local node numbering system.

1, 2, . . . , 8. Each element is considered to have a dimension of h, w, and l in the x, y, and z directions, respectively, as shown.

C. Element Stiffness Matrix

Galerkin's finite element method is used to compute the element stiffness matrix. The field error function is defined as

$$E_r = \nabla^2 p + k^2 p \tag{48}$$

Within each element, p is represented as a linear combination of eight functions, $N_1, N_2, \ldots, N_8$,

$$p = \sum_{m=1}^{m=8} N_m p_m \tag{49}$$

$$N_1 = \left(1 - \frac{x}{h}\right)\left(1 - \frac{y}{w}\right)\left(1 - \frac{z}{l}\right)$$

$$N_2 = \left(1 - \frac{x}{h}\right)\left(\frac{y}{w}\right)\left(1 - \frac{z}{l}\right), \qquad N_3 = \frac{xy}{(w/h)(1 - z/l)}$$

$$N_4 = \left(\frac{x}{h}\right)\left(1 - \frac{y}{w}\right)\left(1 - \frac{z}{l}\right)$$

$$N_5 = \left(1 - \frac{x}{h}\right)\left(1 - \frac{y}{w}\right)\left(\frac{z}{l}\right)$$

$$N_6 = \left(1 - \frac{x}{h}\right)\left(\frac{y}{w}\right)\left(\frac{z}{l}\right), \qquad N_7 = \frac{xyz}{whl}$$

$$N_8 = \left(\frac{x}{h}\right)\left(1 - \frac{y}{w}\right)\left(\frac{z}{l}\right) \tag{50}$$

The linear combination [Eq. (49)] comprises a complete set of basis functions.

For a typical element (I, J, K), contributions to the minimization of the field error function due to local node m over the computational volume V are

$$\int_V E_r N_m \, dV = \int_V [\nabla^2 p + k^2 p] N_m \, dV \tag{51}$$

The second derivative terms in Eq. (51) are reduced to first derivatives using Green's second identity

$$\int_V E_r N_m \, dV = \int_V \left[-\{\nabla\} p \cdot \{\nabla\} N_m + k^2 p N_m\right] dV + \int_S \frac{\partial p}{\partial n} N_m \, dS \tag{52}$$

Elimination of the second derivative terms from the volume integral in Eq. (51) is required so that the linear basis functions N_m can be used. Elimination of the second derivative terms from the volume integral also has the advantage that all impedance boundary conditions can be incorporated into the surface integral of Eq. (52). This allows a choice of basis functions that do not have to satisfy explicitly any impedance boundary conditions. The contribution to the surface integral

$$\int_S \frac{\partial p}{\partial n} N_m \, dS \tag{53}$$

is identically zero for all elements except those that lie along an impedance boundary. Substituting the exit boundary condition [Eq. (47)] into the surface integral in Eq. (53) gives

$$\int_S \frac{\partial p}{\partial n} N_m \, dS = -ik \int_S \frac{p}{\zeta_{\text{exit}}} N_m \, dS \tag{54}$$

along the exit boundary, whereas for elements that lie along the upper, lower, and sidewalls of the duct

$$\int_S \frac{\partial p}{\partial n} N_m \, dS = -ik \int_S \frac{p}{\zeta} N_m \, dS \tag{55}$$

The contribution to the minimization of the field error for each element, when collected for each of the eight local nodes m, is expressed in matrix form as

$$\begin{Bmatrix} \int_V E_r N_1 \, dV \\ \int_V E_r N_2 \, dV \\ \vdots \\ \int_V E_r N_8 \, dV \end{Bmatrix} = \left[A^{(I,J,K)}\right]\left\{\Phi^{(I,J,K)}\right\} \tag{56}$$

In Eq. (56), $\{\Phi^{(I,J,K)}\}$ is an 8×1 column vector for each element containing the unknown acoustic pressures at the eight local nodes of the element

$$\left\{\Phi^{(I,J,K)}\right\}^T = \{p_1, p_2, p_3, p_4, p_5, p_6, p_7, p_8\} \tag{57}$$

The element matrix $[A^{(I,J,K)}]$ is an 8×8 complex symmetric matrix for each element (I, J, K). In the special case of a hard wall duct ($\zeta = \infty$),

$$\left[A^{(I,J,K)}\right] = \begin{Bmatrix} [\mathcal{P}], & K = (NZ - 1) \\ [\mathcal{P}] + [B], & K = (NZ - 1) \end{Bmatrix} \tag{58}$$

Here, $[\mathcal{P}]$ represents the contribution to $[A^{(I,J,K)}]$ due to the element volume V, whereas $[B]$ represents the contributions due to the exit plane boundary. The matrices $[\mathcal{P}]$ and $[B]$ are symmetric, and their coefficients have been computed explicitly:

$$[\mathcal{P}] = \frac{k^2 wlh}{216}[A] - \frac{wl}{36h}[\mathcal{B}] - \frac{hl}{36w}[\mathcal{C}] - \frac{wh}{36l}[\mathcal{F}] \tag{59}$$

$$[A] = \begin{bmatrix} 8 & 4 & 2 & 4 & 4 & 2 & 1 & 2 \\ 4 & 8 & 4 & 2 & 2 & 4 & 2 & 1 \\ 2 & 4 & 8 & 4 & 1 & 2 & 4 & 2 \\ 4 & 2 & 4 & 8 & 2 & 1 & 2 & 4 \\ 4 & 2 & 1 & 2 & 8 & 4 & 2 & 4 \\ 2 & 4 & 2 & 1 & 4 & 8 & 2 & 4 \\ 1 & 2 & 4 & 2 & 2 & 2 & 8 & 4 \\ 2 & 1 & 2 & 4 & 4 & 4 & 4 & 8 \end{bmatrix}$$

$$[\mathcal{B}] = \begin{bmatrix} 4 & 2 & -2 & -4 & 2 & 1 & -1 & -2 \\ 2 & 4 & -4 & -2 & 1 & 2 & -2 & -1 \\ -2 & -4 & 4 & 2 & -1 & -2 & 2 & 1 \\ -4 & -2 & 2 & 4 & -2 & -1 & 1 & 2 \\ 2 & 1 & -1 & -2 & 4 & 2 & -2 & -4 \\ 1 & 2 & -2 & -1 & 2 & 4 & -4 & -2 \\ -1 & -2 & 2 & 1 & -2 & -4 & 4 & 2 \\ -2 & -1 & 1 & 2 & -4 & -2 & 2 & 4 \end{bmatrix} \tag{60}$$

$$[\mathcal{C}] = \begin{bmatrix} 4 & -4 & -2 & 2 & 2 & -2 & -1 & 1 \\ -4 & 4 & 2 & -2 & -2 & 2 & 1 & -1 \\ -2 & 2 & 4 & -4 & -1 & 1 & 2 & -2 \\ 2 & -2 & -4 & 4 & 1 & -1 & -2 & 2 \\ 2 & -2 & -1 & 1 & 4 & -4 & -2 & 2 \\ -2 & 2 & 1 & -1 & -4 & 4 & 2 & -2 \\ -1 & 1 & 2 & -2 & -2 & 2 & 4 & -4 \\ 1 & -1 & -2 & 2 & 2 & -2 & -4 & 4 \end{bmatrix} \tag{61}$$

$$[\mathcal{F}] = \begin{bmatrix} 4 & 2 & 1 & 2 & -4 & -2 & -1 & -2 \\ 2 & 4 & 2 & 1 & -2 & -4 & -2 & -1 \\ 1 & 2 & 4 & 2 & -1 & -2 & -4 & -2 \\ 2 & 1 & 2 & 4 & -2 & -1 & -2 & -4 \\ -4 & -2 & -1 & -2 & 4 & 2 & 1 & 2 \\ -2 & -4 & -2 & -1 & 2 & 4 & 2 & 1 \\ -1 & -2 & -4 & -2 & 1 & 2 & 4 & 2 \\ -2 & -1 & -2 & -4 & 2 & 1 & 2 & 4 \end{bmatrix} \tag{62}$$

$$[B] = -ik\frac{wl}{72} \begin{bmatrix} 0 & 0 & 0 & 0 & 0 & 0 & 0 & 0 \\ 0 & 0 & 0 & 0 & 0 & 0 & 0 & 0 \\ 0 & 0 & 0 & 0 & 0 & 0 & 0 & 0 \\ 0 & 0 & 0 & 0 & 0 & 0 & 0 & 0 \\ 0 & 0 & 0 & 0 & f_1 & f_2 & f_3 & f_4 \\ 0 & 0 & 0 & 0 & f_2 & f_5 & f_6 & f_7 \\ 0 & 0 & 0 & 0 & f_3 & f_6 & f_7 & f_8 \\ 0 & 0 & 0 & 0 & f_4 & f_7 & f_8 & f_9 \end{bmatrix} \tag{63}$$

$$f_1 = 9\beta_{\text{exit}}(x_I, y_J) - 3\beta_{\text{exit}}(x_I, y_{J+1}) + \beta_{\text{exit}}(x_{I+1}, y_{J+1}) + 3\beta_{\text{exit}}(x_I, y_{J+1})$$

$$f_2 = 3\beta_{\text{exit}}(x_I, y_J) - \beta_{\text{exit}}(x_I, y_{J+1})] + \beta_{\text{exit}}(x_{I+1}, y_{J+1}) + \beta_{\text{exit}}(x_I, y_{J+1})$$

$$f_3 = \beta_{\text{exit}}(x_I, y_J) + \beta_{\text{exit}}(x_I, y_{J+1}) + \beta_{\text{exit}}(x_{I+1}, y_{J+1}) + \beta_{\text{exit}}(x_I, y_{J+1})$$

$$f_4 = 3\beta_{\text{exit}}(x_I, y_J) + \beta_{\text{exit}}(x_I, y_{J+1}) - \beta_{\text{exit}}(x_{I+1}, y_{J+1}) + 3\beta_{\text{exit}}(x_I, y_{J+1})$$

$$f_5 = 3\beta_{\text{exit}}(x_I, y_J) + 9\beta_{\text{exit}}(x_I, y_{J+1}) - 3\beta_{\text{exit}}(x_{I+1}, y_{J+1}) + \beta_{\text{exit}}(x_I, y_{J+1})$$

$$f_6 = \beta_{\text{exit}}(x_I, y_J) + 3\beta_{\text{exit}}(x_I, y_{J+1}) - 3\beta_{\text{exit}}(x_{I+1}, y_{J+1}) + \beta_{\text{exit}}(x_I, y_{J+1})$$

$$f_7 = \beta_{\text{exit}}(x_I, y_J) + 3\beta_{\text{exit}}(x_I, y_{J+1}) - 9\beta_{\text{exit}}(x_{I+1}, y_{J+1}) + 3\beta_{\text{exit}}(x_I, y_{J+1})$$

$$f_8 = \beta_{\text{exit}}(x_I, y_J) + \beta_{\text{exit}}(x_I, y_{J+1}) - 3[\beta_{\text{exit}}(x_{I+1}, y_{J+1}) + \beta_{\text{exit}}(x_I, y_{J+1})]$$

$$f_9 = 3\beta_{\text{exit}}(x_I, y_J) + \beta_{\text{exit}}(x_I, y_{J+1}) - 3\beta_{\text{exit}}(x_{I+1}, y_{J+1}) + 9\beta_{\text{exit}}(x_I, y_{J+1}) \tag{64}$$

in which

$$\beta_{\text{exit}} = 1/\zeta_{\text{exit}} \tag{65}$$

V. Results and Discussion

The three-dimensional rigid wall acoustic element has been coupled with the sparse assembly and equation solver algorithms to provide assembly and solver statistics for a three-dimensional duct aeroacoustics application. Computations presented in this paper were run on a single processor with double-precision (64-bit) arithmetic on an ORIGIN 2000 computer platform. The sparse equation solver used MMD reordering. Computations are presented for a uniform grid and a geometry identical to that of the Langley Flow Impedance Tube. This three-dimensional duct has a square cross section 0.0508 m in width ($W = H = 0.0508$ m) and 0.812 m in length ($L = 0.812$ m). A more detailed description of the duct is given in Ref. 15. All calculations were performed at standard atmospheric conditions without flow, and the source frequency was chosen to span the full range of frequencies currently of interest in duct liner research. The sound was chosen as a plane wave ($p_s = 1$), and the dimensionless exit impedance was chosen as unity ($\zeta_{\text{exit}} = 1$). This exit impedance will simulate a nonreflecting termination for the plane wave source.

Table 1 presents CPU statistics (in seconds) for each of the three assembly algorithms and the sparse equation solver as a function of the source frequency f, in kilohertz. The CPU time for the solver (column 9) is that required to obtain the solution vector after the system matrix was assembled. Note that before obtaining the solution vector, the system matrices obtained from each assembly algorithm were compared to each other. Each assembly algorithm assembled the identical system matrix as expected. Also included in Table 1 are the number of grid lines NX, NY, and NZ and the matrix order N that were used to perform the computations at each frequency. Here we have used the generally accepted rule that 12 points per wavelength is required to resolve a cut-on mode in each coordinate direction. To establish the accuracy of the solver solutions, the relative error norm (Relerr), computed from the solver solution vector, was tabulated in the final column of Table 1. The relative error norm[2] is defined as

$$\text{Relerr} = \frac{\{EN\}^* \times \{EN\}^T}{\{\bar{F}\}^* \times \{\bar{F}\}^T} \tag{66}$$

where

$$\{EN\} = [\bar{A}]\{\Phi\} - \{\bar{F}\} \tag{67}$$

f	NX	NY	NZ	N	Algorithm 1	Algorithm 2	Algorithm 3	Solver	Relerr
4.00	6	6	114	4,104	49.20	0.34	0.22	6.00	6.5×10^{-15}
7.00	12	12	200	28,800	106.80	2.50	1.75	22.80	1.8×10^{-12}
11.00	18	18	313	101,412	1,123.80	9.05	2.28	487.80	7.5×10^{-12}
14.00	24	24	399	229,824	5,520.60	20.74	14.24	3,120.00	3.4×10^{-11}
17.00	30	30	484	435,600	19,488.00	39.78	26.94	10,440.00	3.2×10^{-11}
21.00	36	36	599	776,304	N/A	73.81	48.35	N/A	N/A

669

Table 2 RAM statistics (in megabytes) for the sparse algorithms

f	N	NI	Algorithm 2	Algorithm 3	Solver
4.00	4,104	41,468	0.47	0.46	4.00
7.00	28,800	331,244	21.00	11.00	80.00
11.00	101,412	1,216,118	72.00	37.00	640.00
14.00	229,824	2,812,838	165.00	83.00	2,140.00
17.00	435,600	5,396,600	317.00	158.00	8,100.00
21.00	776,304	9,696,158	551.00	283.00	N/A

Tabular results at 21 kHz are not presented for assembly algorithm 1 and the sparse equation solver because of the excessive CPU time required by these two algorithms.

Although algorithm 1 is extremely simple, its performance is extremely slow (Table 1). Note that algorithm 1 is 145 times slower than the other two algorithms at a frequency of 4 kHz and more than 490 times slower at 17 kHz. Tabular results also show that the CPU time required to assemble the system matrix using algorithm 1 exceeds that required to obtain the solution vector by 9048 s (or 87%) at 17 kHz. At low frequencies, algorithm 2 is only slightly slower than algorithm 3, but as the frequency increases to 17 kHz, algorithm 3 is 32% faster than algorithm 2. Generally, the higher the frequency, the better the performance of algorithm 3, relative to that of algorithm 2. Furthermore, in using algorithm 2, the user has to guess the maximum number of nonzero terms per row (MZ) to allocate the RAM for the matrix $[IA]$. Also, the CPU times required to assemble the system matrix using algorithm 2 or algorithm 3 are both more than two orders of magnitude less than the time required to obtain the solution vector. Finally, Relerr is small, indicating that the solver solution is accurate.

Table 2 shows the RAM (in megabytes) for algorithm 2, algorithm 3, and the sparse equation solver. RAM statistics for algorithm 1 were not tabulated because its performance was extremely slow when compared to algorithm 2 and algorithm 3 (as shown in Table 1). Values of the variables N and NI are also given in Table 2. The results show that the number of off-diagonal nonzero coefficients (NI) is an order of magnitude larger than N. Table 2 also shows that algorithm 3 requires less memory than algorithm 2 because algorithm 2 must allocate RAM for storing vectors $[IR]$, $[JC]$, and $[HA]$ [see Eqs. (13–15)]. Note also that memory required by the sparse equation solver is substantially larger than that required for assembly algorithm 2 or algorithm 3. This is further verification that most of the RAM allocated is used during matrix factorization. Preliminary results from tests conducted by the authors have suggested that the performance of the sparse equation solver may improve if the solver were to use METIS instead of MMD reordering. For example, at 7 kHz the number of nonzeros after factorization (NZ) was reduced from 4,736,991 with MMD reordering to only 4,376,496 when the METIS reordering algorithm was used.

VI. Conclusions

A template for symmetric sparse equation assembly and solutions on an unstructured grid has been presented. The accuracy and numerical performance of the sparse algorithms have been evaluated over the frequency range of interest in a three-dimensional aeroacoustics application. Based on the results of this study, the following conclusions are drawn:

1) Assembly algorithm 1 is impractical for system matrix assembly at high values of source frequency. It requires up to 87% more CPU time to assemble the system matrix than the sparse equation solver requires to obtain the solution vector.

2) Assembly algorithms 2 and 3 have nearly equal performances at low values of source frequency, but algorithm 3 gives savings in both CPU time (32%) and RAM (50%) at the higher values of source frequency.

3) Error norm statistics show that the sparse equation solver computes accurate acoustic solutions over the frequency range of interest for the three-dimensional aeroacoustics application.

4) At high frequency (17 kHz), the sparse equation solver requires low memory, but requires significant speed-up before optimization studies (either of the duct geometry or liner material properties) are practical. This research supports a recommendation, therefore, that a parallel version of the sparse solver be developed. The CPU time and RAM required by assembly algorithms 2 and 3 are two orders of magnitude smaller than that required by the sparse equation solver. These algorithms can, therefore, be conveniently incorporated into a substructuring (or domain decomposition) formulation (provided that each substructure is handled by different processors) to take advantage of parallel computation to further reduce CPU time and RAM.

References

[1]Stead, D., "A Best Choice Numerical Method for Large-Scale Computations in Aeroacoustics," M.S. Thesis, Joint Inst. of Acoustics and Flight Science, George Washington Univ., Hampton, VA, June 1999.

[2]Nguyen, D., *Parallel-Vector Equation Solvers for Finite Element Engineering Applications*, Kluwer/Plenum, Norwell, MA, 2001, Chap. 10.

[3]Nguyen, D., Hou, G., Runesha, H., and Han, B., "Alternative Approach for Solving Sparse Indefinite Symmetrical System of Equations," *Advances in Engineering Software*, Vol. 31, Nos. 8–9, 2000, pp. 581–584.

[4]Chen, P., Runesha, H., Nguyen, D., Tong, P., and Chang, T., "Sparse Algorithms for Indefinite Systems of Linear Equations," *Computational Mechanics Journal*, Vol. 25, No. 1, 2000, pp. 33–41.

[5]George, A., and Liu, J., *Computer Solution of Large Sparse Positive Definite Systems*, Prentice–Hall, Englewood Cliffs, NJ, 1981, Chaps. 5 and 10.

[6]Pissanetzsky, S., "Gauss Elimination with Supersparse Matrices," Brookhaven National Lab., Rept. BNL 26773, Upton, NY, 1979.

[7]Simon, H., Vu, P., and Yang, C., "Performance of a Supernodal General Sparse Solver on the Cray-YMP: 1.68 GFLOPS with Autotasking," Applied Mathematics TR, Boeing Computer Services, SCA-TR-117, Seattle, WA, March 1989.

[8]Liu, J., "The Role of Elimination Trees in Sparse Factorization," *SIAM Journal of Matrix Analysis Application*, Vol. 11, No. 1, 1990, pp. 134–172.

[9]Duff, I., and Reid, J., "MA27-A Set of Fortran Subroutines for Solving Sparse Symmetric Sets of Linear Equations," Atomic Energy Research Establishment, TR R-10533, Harwell, England, U.K., 1982.

[10]Duff, I., and Reid, J., "The Multifrontal Solution of Indefinite Sparse Symmetric Linear Systems," *Association for Computing Machinery Transactions Mathematical Software*, Vol. 9, No. 3, 1983, pp. 302–325.

[11]Duff, I., Gould, N., Reid, J., Scott, J., and Turner, K., "Factorization of Sparse Symmetric Indefinite Matrices," *Institute of Mathematics and Its Applications Journal of Numerical Analysis*, Vol. 11, No. 9, 1991, pp. 181–204.

[12]Duff, I., Grimes, R., and Lewis, J., "Users' Guide for the Harwell–Boeing Sparse Matrix Collection (Release I)," Rutherford Appleton Lab., TR 92-086, Chilton, England, U.K., 1992.

[13]Duff, I., and Reid, J., "MAAT, a Fortran Code for Direct Solution of Indefinite Sparse Symmetric Linear Systems," Rutherford Appleton Lab., RAL-95-001, Chilton, England, U.K., Jan. 1995.

[14]Ng, E., and Peyton, B., "Block Sparse Choleski Algorithm on Advanced Uniprocessor Computer," *SIAM Journal of Scientific Computing*, Vol. 14, No. 5, 1993, pp. 1034–56.

[15]Watson, W., "Three-Dimensional Nacelle Aeroacoustic Code with Application to Impedance Eduction," AIAA Paper 2000-1956, June 2000.

[16]Chandrakant, S., and Abel, J., *Introduction to the Finite Element Method*, Van Nostrand Reinhold, New York, 1972, pp. 75–147.

670

[17]Ashcraft, C., "Compressed Graphs and the Minimum Degree Algorithm," *SIAM Journal of Scientific Computing*, Vol. 16, No. 6, 1995, pp. 1404–411.

[18]Gamma, E., Helm, R., Johnson, R., and Vlissides, J., "Design Patterns: Elements of Reusable Object-Oriented Software," *Addison Wesley Professional Computing Series*, Addison Wesley Longman, Reading, MA, 1995, pp. 25–30.

[19]George, J., and Liu, J., "The Evolution of the Minimum Degree Algorithm," *Society for Industrial and Applied Mathematics*, Vol. 31, No. 1, 1989, pp. 1–19.

[20]Liu, J., "Modification of the Minimum-Degree Algorithm by Multiple Elimination," *Association for Computing Machinery, Transactions on Mathematical Software*, Vol. 11, No. 2, 1985, pp. 141–53.

[21]Kumfert, G., and Pothen, A., "An Object-Oriented Collection of Minimum Degree Algorithms: Design, Implementation, and Experiences," NASA CR-1999-208977 1999; also Inst. for Computer Applications in Science and Engineering, Rept. 99-1, Hampton, VA, Jan. 1999.

[22]Amestoy, P., Davis, T., and Duff, I., "An Approximate Minimum Degree Ordering Algorithm," Computer and Information Science Dept., TR-94-039, Univ. of Florida, Gainesvine, FL, Dec. 1994.

[23]Karypis, G., and Kumar, V., "METIS: Unstructured Graph Partitioning and Sparse Matrix Ordering," Ver. 2.0, Univ. of Minnesota, Minneapolis, MN, 1995.

[24]Runesha, H., and Nguyen, D., "Vectorized Sparse Unsymmetrical Equation Solver for Computational Mechanics," *Advances in Engineering Software*, Vol. 31, Nos. 8–9, 2000, pp. 563–570.

P. J. Morris
Associate Editor

Fundamentals of Kalman Filtering: A Practical Approach

Paul Zarchan and Howard Musoff, C.S. Draper Laboratory

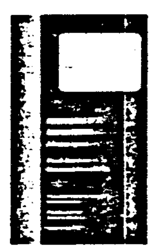

This text is a practical guide to building Kalman filters and shows how the filtering equations can be applied to real-life problems. Numerous examples are presented in detail showing the many ways in which Kalman filters can be designed. Computer code written in FORTRAN, MATLAB, and True BASIC accompanies all of the examples so that the interested reader can verify concepts and explore issues beyond the scope of the text. Sometimes mistakes are introduced intentionally to the initial filter designs to show the reader what happens when the filter is not working properly. The text spends a great deal of time setting up a problem before the Kalman filter is actually formulated to give the reader an intuitive feel for the problem being addressed. Real problems are seldom presented in the form of differential equations and they usually don't have unique solutions. Therefore, the authors illustrate several different filtering approaches for tackling a problem. Readers will gain experience in software and performance tradeoffs for determining the best filtering approach for the application at hand.

Progress in Astronautics and Aeronautics
2000, 670 pp, Hardcover
ISBN 1-56347-455-7
List Price: $99.95
AIAA Member Price: $74.95
Source: **945**

AIAA
American Institute of Aeronautics and Astronautics
Publications Customer Service, 9 Jay Gould Ct., P.O. Box 753, Waldorf, MD 20604
Fax 301/843-0159, Phone 800/682-2422, E-mail aiaa@tasco1.com
8 am–5 pm Eastern Standard Time
Order 24 hours a day at www.aiaa.org

CA and VA residents add applicable sales tax. For shipping and handling add $4.75 for 1–4 books (call for rates for higher quantities). All individual orders—including U.S., Canadian, and foreign—must be prepaid by personal or company check, traveler's check, international money order, or credit card (VISA, MasterCard, American Express, or Diners Club). All checks must be made payable to AIAA in U.S. dollars, drawn on a U.S. bank. Orders from libraries, corporations, government agencies, and university and college bookstores must be accompanied by an authorized purchase order. All other bookstore orders must be prepaid. Please allow 4 weeks for delivery. Prices are subject to change without notice. Returns in sellable condition will be accepted within 30 days. Sorry, we cannot accept returns of case studies, conference proceedings, sale items, or software (unless defective). Non-U.S. residents are responsible for payment of any taxes required by their government.

01-0344

3. Parallel Finite Element Domain Decomposition for Structural/ Acoustic Analysis: Symmetrical Case [Ref. 6.2]

(Please refer to the attached Journal Paper for this section)

Journal of Computational and Applied Mechanics, Vol. 4., No. 2., (2003), pp. 189–201

PARALLEL FINITE ELEMENT DOMAIN DECOMPOSITION FOR STRUCTURAL/ACOUSTIC ANALYSIS

DUC T. NGUYEN, SIROJ TUNGKAHOTARA
Department of Civil and Environmental Engineering, 135 KAUF Hall
Old Dominion University, Norfolk, VA 23529, USA
dnguyen@odu.edu, toohtaah@yahoo.com

WILLIE R. WATSON
Computational Modelling & Simulation Branch, MS 128
NASA Langley Research Center, Hampton, VA 23681, USA
w.r.watson@larc.nasa.gov

SUBRAMANIAM D. RAJAN
Civil Engineering Department, ECG 252
Arizona State University, Tempe, AZ 85287, USA
s.rajan@asu.edu

[Received: July 24, 2002]

Abstract. A domain decomposition (DD) formulation for solving sparse linear systems of equations resulting from finite element analysis is presented. The formulation incorporates mixed direct and iterative equation solving strategies and other novel algorithmic ideas that are optimized to take advantage of sparsity and exploit modern computer architecture, such as memory and parallel computing. The most time consuming part of the formulation is identified and the critical roles of direct sparse and iterative solvers within the framework of the formulation are discussed. Experiments on several computer platforms using real and complex test matrices are conducted using software based on the formulation. Small-scale structural examples are used to validate the steps in the formulation and large-scale (1,000,000+ unknowns) duct acoustic examples are used to evaluate the parallel performance of the formulation. Results are presented using 64 SUN 10000, 8 SGI ORIGIN 2000 processors, and a cluster of 6 PCs (running under the Windows environment). Statistics show that the formulation is efficient in both sequential and parallel computing environments and that the formulation is significantly faster and consumes less memory than that based on one of the best available commercialized parallel sparse solvers.

Mathematical Subject Classification: 74S05,15A06,
Keywords: linear algebra, sparse matrix computation, parallel computation, finite element, domain decomposition, structures, acoustics

1. Domain decomposition (DD) formulation for finite element analyses

Application of finite element analysis to engineering problems leads to the discrete equation system [1, 2]

$$[K]\{Z\} = \{S\}\,. \tag{1.1}$$

where S, Z are vectors of length N that contains the known nodal loads and unknown nodal quantities, respectively. Here K is a complex, nonsingular, symmetric/unsymmetric, NxN sparse matrix. Although (1.1) assumes a single loading condition (i.e., right hand side), multiple loading conditions may be treated by taking S and Z as dense matrices, so that the j^{th} column of Z corresponds to the N unknown nodal quantities associated with the loadings in the j^{th} column of S.

Using the domain decomposition concept, (1.1) is written in partitioned form

$$\begin{bmatrix} K_{BB} & K_{BI} \\ K_{IB} & K_{II} \end{bmatrix} \begin{Bmatrix} Z_B \\ Z_I \end{Bmatrix} = \begin{Bmatrix} S_B \\ S_I \end{Bmatrix} \tag{1.2}$$

where submatrices K_{IB}, K_{BI}, K_{II} and K_{BB} have dimension mxn, nxm, mxm and nxn, respectively. The interior and boundary unknowns (i.e., Z_I and Z_B) have dimensions compatible with the columns in K_{II} and K_{BB}, respectively.

Eliminating the interior unknowns from (1.2) gives

$$K_B Z_B = F_B \,, \tag{1.3}$$

where

$$K_B = K_{BB} + K_{BI} Q \,, \tag{1.4}$$

$$Q = -K_{II}^{-1} K_{IB} \,, \tag{1.5}$$

$$F_B = S_B + \bar{Q} \,, \tag{1.6}$$

$$\bar{Q} = -K_{BI} \bar{S}_I \,, \tag{1.7}$$

$$\bar{S}_I = K_{II}^{-1} S_I \,. \tag{1.8}$$

Here K_B is the boundary stiffness matrix for the domain, F_B is the vector of boundary forces, and the superscript (i.e., -1) denotes the matrix inverse. Efficient sparse algorithm [3]-[11] may be used to decompose sparse matrix K_{II} and solve for matrix Q in (1.5) and the vector $\bar{S}_I$ in (1.8).

In the current DD formulation [12, 13] the computational domain is decomposed into L subdomains and K_B and F_B are synthesized by considering contributions from all subdomains. For this purpose, the discrete equation system for a subdomain (which is considered an isolated free-body) is expressed in the form (1.2)

$$\begin{bmatrix} K_{BB}^{(r)} & K_{BI}^{(r)} \\ K_{IB}^{(r)} & K_{II}^{(r)} \end{bmatrix} \begin{Bmatrix} Z_B^{(r)} \\ Z_I^{(r)} \end{Bmatrix} = \begin{Bmatrix} S_B^{(r)} \\ S_I^{(r)} \end{Bmatrix}, \quad r = 1, 2, 3 \cdots L \tag{1.9}$$

where r refers to the r^{th} subdomain. Let $n^{(r)}$ and $m^{(r)}$ represent the number of boundary and interior unknowns of the r^{th} subdomain, respectively. The solution of (1.9) is

$$K_B^{(r)} Z_B^{(r)} = F_B^{(r)} \,, \tag{1.10}$$

$$Z_I^{(r)} = (K_{II}^{(r)})^{-1} (S_I^{(r)} - K_{IB}^{(r)} Z_B^{(r)}) \,. \tag{1.11}$$

where

$$K_B^{(r)} = K_{BB}^{(r)} + K_{BI}^{(r)} Q^{(r)} \,, \tag{1.12}$$

$$Q^{(r)} = -(K_{II}^{(r)})^{-1} K_{IB}^{(r)} \,, \tag{1.13}$$

$$F_B^{(r)} = S_B^{(r)} + \tilde{Q}^{(r)} , \tag{1.14}$$

$$\tilde{Q}^{(r)} = -K_{BI}^{(r)} \tilde{S}_I^{(r)} , \tag{1.15}$$

$$\tilde{S}_I^{(r)} = (K_{II}^{(r)})^{-1} S_I^{(r)} . \tag{1.16}$$

Finally, K_B and F_B may be obtained explicitly from the equations

$$K_B = \sum_{r=1}^{L} (\beta^{(r)})^T K_B^{(r)} \beta^{(r)} , \qquad F_B = S_B + \sum_{r=1}^{L} (\beta^{(r)})^T (Q^{(r)})^T S_I^{(r)} , \tag{1.17}$$

where $\beta^{(r)}$ is a Boolean transformation matrix of dimension $n^{(r)} \times n^{(r)}$.

The sequence of steps constituting the DD formulation proposed in this paper is as follows:

(1) Decompose the large-scale finite element domain into L smaller subdomains. Algorithms and software given in [12, 13] are used for this purpose.
(2) Compute $K_{IB}^{(r)}, K_{BI}^{(r)}, K_{II}^{(r)}, K_{BB}^{(r)}, S_B^{(r)}$, and $S_B^{(r)}$ using efficient sparse assembly algorithms [3, 11].
(3) Factorize the sparse matrix $K_{II}^{(r)}$ and compute $\tilde{S}_I^{(r)}$ using (1.16) and $Q^{(r)}$ using (1.13). Algorithms and software for sparse symbolic and numerical factorization, loop unrolling techniques, equation reordering, and forward-backward solution phases ([3]-[11]) are utilized at this step.
(4) Compute $K_B^{(r)}$ and $F_B^{(r)}$ for each subdomain.
(5) Compute K_B and F_B from (1.17).
(6) Solve (1.3) using a direct or iterative solver to obtain the boundary unknowns, Z_B.
    a): Efficient parallel direct dense solvers given in [14]-[16] may be utilized at this step provided that K_B is formed explicitly.
    b): However, explicit computation of K_B is an expensive operation due to the need to perform the inner produce $K_{BI}^{(r)} Q^{(r)}$ in (1.12).
    c): Iterative solvers (such as the preconditioned conjugate gradient algorithm) [17] are therefore recommended for this step in the formulation. The use of an iterative solver eliminates the need to form K_B explicitly because each stage of the iterative solution typically requires only the product a matrix $(K_{BB} + K_{BI}^{(r)}) Q^{(r)}$ with a known vector.
(7) Finally, the solution for the interior unknowns are obtained from (1.11) by using the factorized sparse matrix $K_{II}^{(r)}$ during the forward and backward substitution phases.

The solution vectors obtained from the formulation are post-processed to obtain other quantities of interest such as stresses, strains, acoustic energy, etc. The remaining sections of this paper will focus on issues related to efficient sparse assembly procedures.

2. Simple finite element model

To facilitate the discussion a simple finite element model which consists of 4 rectangular elements with 1 degree of freedom (dof) per node and its loading condition

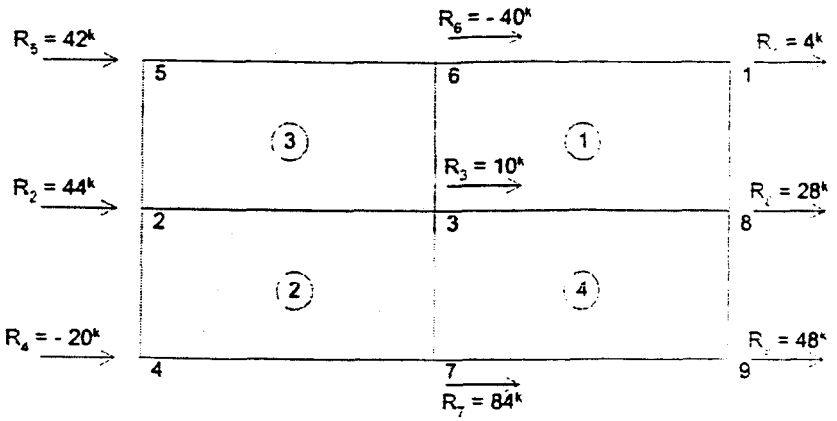

Figure 1. A simple unconstrained finite element model

(R_i) is shown in Figure 1. The global dof associated with each of the e^{th} rectangular element in Figure 1 are given by the following "element-dof" connectivity matrix, E

$$[E] = \begin{array}{c|ccccccccc} & 1 & 2 & 3 & 4 & 5 & 6 & 7 & 8 & 9 \\ \hline 1 & x & & x & & & x & & x & \\ 2 & & x & x & x & & & x & & \\ 3 & & x & x & & x & x & & & \\ 4 & & & x & & & & x & x & x \end{array} . \tag{2.1}$$

The number of rows and columns in E correspond to the total number of finite elements (4 finite elements) and degrees of freedom (9 dof), in the model. The following 2 integer arrays describe the nonzero structure of E in a row oriented format

$$\{IE\}^T = \{1, 5, 9, 13, 17\} , \tag{2.2}$$

$$\{JE\}^T = \{3, 8, 1, 6, 7, 3, 2, 4, 5, 2, 3, 6, 7, 9, 8, 3\} . \tag{2.3}$$

The array IE contains the starting location of the first nonzero terms for each row of matrix E while JE contains the global dof number associated with each e^{th} (e=1,2,3,4) rectangular element. This format is called compress row format. Similarly, the transpose of the matrix E can be described by two integer arrays, IET and JET.

The "exact" numerical values for the 4x4 element stiffness matrix $K^{(e)}$ is "unimportant" at this stage of the discussions and are assumed to be given by the following formulas:

$$[K^{(1)}] = \begin{array}{|cccc|c|} \multicolumn{4}{c}{3\ \ 8\ \ 1\ \ 6} & \\ \hline 2 & 3 & 4 & 5 & 3 \\ -3 & 4 & 5 & 6 & 8 \\ -4 & -5 & 6 & 7 & 1 \\ -5 & -6 & -7 & 8 & 6 \\ \hline \end{array} \qquad [K^{(2)}] = \begin{array}{|cccc|c|} \multicolumn{4}{c}{7\ \ 3\ \ 2\ \ 4} & \\ \hline 4 & 6 & 8 & 10 & 7 \\ -6 & 8 & 10 & 12 & 3 \\ -8 & -10 & 12 & 14 & 2 \\ -10 & -12 & -14 & 16 & 4 \\ \hline \end{array} \tag{2.4}$$

$$[K^{(3)}] = \begin{array}{|cccc|c|} \multicolumn{4}{c}{5\ \ 2\ \ 3\ \ 6} & \\ \hline 6 & 9 & 12 & 15 & 5 \\ -9 & 12 & 15 & 18 & 2 \\ -12 & -15 & 18 & 21 & 3 \\ -15 & -18 & -21 & 24 & 6 \\ \hline \end{array} \qquad [K^{(4)}] = \begin{array}{|cccc|c|} \multicolumn{4}{c}{7\ \ 9\ \ 8\ \ 3} & \\ \hline 8 & 12 & 16 & 20 & 7 \\ -12 & 16 & 20 & 24 & 9 \\ -16 & -20 & 24 & 28 & 8 \\ -20 & -24 & -28 & 32 & 3 \\ \hline \end{array} \tag{2.5}$$

Note that the global row and column numbers for the e^{th} rectangular element are easily obtained from JE. For example, the global row and column numbers 7,3,2, and 4 for rectangular element 2, are contained in the 5,6,7, and 8^{th} element of JE. Further, the "simulated" element stiffness matrices, $K^{(e)}$, are unsymmetrical in value but symmetrical in locations. For example, $K^{(2)}$ has a nonzero term of 14 at location (3,4), and there is also a nonzero term of -14 at location (4,3). Following the usual finite element procedures, the system of linear unsymmetrical equations for the finite element model shown in Figure 1 can be assembled as

$$[K]\{Z\} = \{S\}\,, \tag{2.6}$$

where

$$[K] = \sum_{e=1}^{4} [K]^{(e)}\,. \tag{2.7}$$

For example, $K_{3,3} = K^{(1)}_{3,3} + K^{(2)}_{3,3} + K^{(3)}_{3,3} + K^{(4)}_{3,3} = 2 + 8 + 18 + 32 = 60$ as indicated in (2.8)

$$[K] = \begin{array}{|ccccccccc|c|} \multicolumn{9}{c}{1\ \ 2\ \ 3\ \ 4\ \ 5\ \ 6\ \ 7\ \ 8\ \ 9} & \\ \hline 6 & & -4 & & & 7 & & -5 & & 1 \\ & 24 & 5 & 14 & -9 & 18 & -8 & & & 2 \\ 4 & -5 & 60 & 12 & -12 & 26 & -26 & -25 & -24 & 3 \\ & -14 & -12 & 16 & F & F & -10 & F & F & 4 \\ & 9 & 12 & & 6 & 15 & F & F & F & 5 \\ -7 & -18 & -26 & & -15 & 32 & F & -6 & F & 6 \\ & 8 & 26 & 10 & & & 12 & 16 & 12 & 7 \\ 5 & & 25 & & & 6 & -16 & 28 & -20 & 8 \\ & & 24 & & & & -12 & 20 & 16 & 9 \\ \hline \end{array} \tag{2.8}$$

$$\{S\}^T = \{4.44, 10., -20.42, -40.84, 28.48\}\,, \tag{2.9}$$

where F represents fill-in terms (shown in the upper triangular portion of matrix K only) that occur during factorization of K.

The solution to equation (2.6) is:

$$\{Z\}^T = \{1,1,1,1,1.1.1.1.1\} \tag{2.10}$$

which has been independently confirmed by the results of the computer program developed. In the upper triangular portion of K. there are 9 fill-in terms. In order to minimize the number of fill-in terms during the symbolic and numerical factorization phases, reordering algorithms [10, 13] such as multiple minimum degree (MMD), Nested-dissection (ND), and METIS are used in the DD formulation.

3. Symbolic sparse assembly for symmetrical and unsymmetrical matrices

It is useful to understand the symbolic sparse assembly for "symmetrical" matrices [3, 11] before proceeding to the unsymmetrical case. Figure 2 gives a "pseudo"

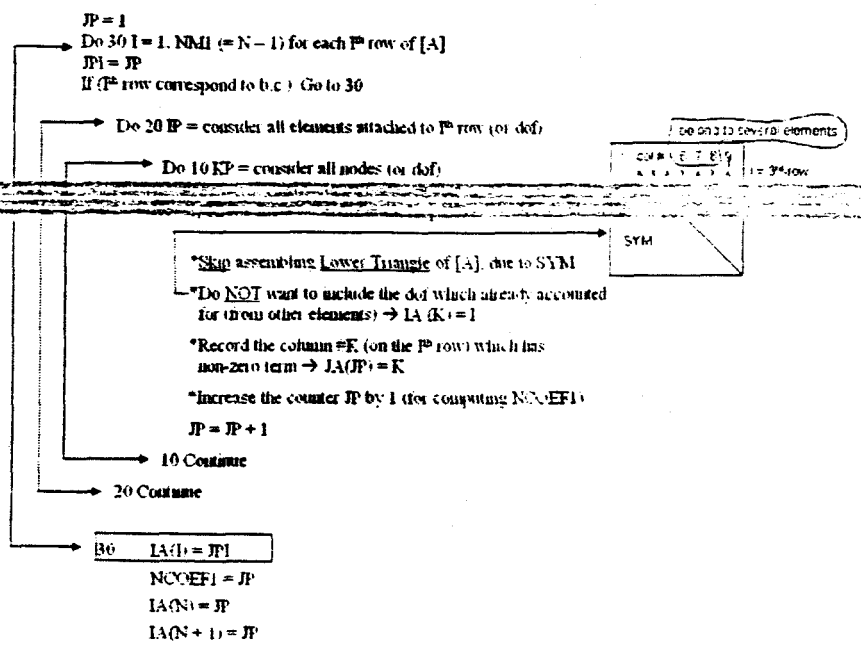

Figure 2. Pseudo Fortran codes for symmetrical symbolic sparse assembly

Fortran coding of the symmetrical sparse assembly procedure. Only minor changes in this symmetrical assembly procedure are required to extend it to unsymmetrical matrices.

In a symmetric matrix the "lower triangular" portion of K is identical with the "upper triangular portion." Thus, the upper triangular portion of K (neglecting fill-in terms (2.8)) can be represented in compressed row format by the following 2 integer arrays:

$$\{IA\}^T = \{1,4,9,15,16,17.18.20.21.21\}\ . \tag{3.1}$$

$$\{JA\}^T = \{3, 6, 8, 3, 4, 5, 6, 7, 4, 5, 6, 7, 8, 9, 7, 6, 8, 8, 9, 9\} \,. \tag{3.2}$$

where the array IA contain the starting location of the first non-zero, off-diagonal term for each row of the upper triangular portion of K. The difference between any 2 consecutive integers on the right-hand-side of (3.1) will give the number of non-zero (off-diagonal) terms in a particular row of the upper triangular portion of K. For example, IA(3)-IA(2) = 9-4 = 5. Hence, there are 5 non-zero terms (excluding the diagonal)) in row 2 of the upper triangular portion of matrix K. Additionally, JA contains the column numbers, associated with each non-zero, off-diagonal term for each row of the upper triangular portion of matrix K. Note that IA and JA arrays can also be obtained from the "pseudo" Fortran coding shown in Figure 2.

The following minor changes in the coding of Figure 2 are required to perform unsymmetrical assembly.

a): DO 30 I= 1, N (the last row will NOT be skipped)
b): Introduce a new integer array IAKEEP(N+1) which plays the role of array IA(-), for example: IAKEEP(I)= JPI .
c): Remove the IF statement in Figure 2 that skips the lower triangular portion. As a consequence of this, the original array IA (-) will contain some additional, unwanted terms.
d): The output from the "unsymmetrical" sparse assembly will be stored by IAKEEP(-) and JA(-), instead of IA(-) and JA(-) as in the symmetrical case.

4. Applications

4.1. Software. The software that is based on the parallel DD formulation presented in this paper has been developed. The parallel algorithm uses the message passing interface (MPI) for interprocess communication and is therefore highly portable. The software developed is referred to as the direct iterative parallel sparse solver (DIPSS). DIPSS (in FORTRAN) incorporates a number of lower level routines and provides options for both real and complex matrices in double precision (i.e., 64-bit arithmetic). Results are presented for symmetric matrices only. We use sparse factorization techniques presented in [3] and implement the preconditioned conjugate gradient iterative solver [17] to solve the dense system (1.3). The following three examples are used to evaluate the proposed parallel DD formulation. Performance gains are particularly evident for large problems.

4.2. Example 1– Mixed finite element types. This is a structural example for which the equation system is real and symmetric and has more than 1 finite element type. The entire finite element model is shown in Figure 3 and consists of 2-node "line" elements, 3-node "triangular" elements, and 4-node "rectangular" elements. Interior and boundary nodes are denoted by open and filled circles, respectively. This small-scale, finite element model is decomposed into 3 subdomains as indicated in Figure 4. The primary purpose of this example is to validate all intermediate and

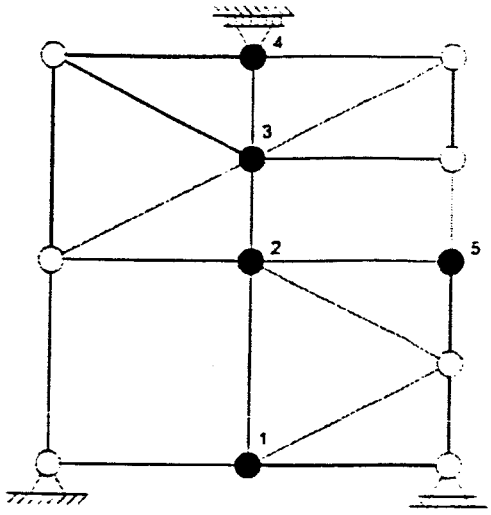

Figure 3. Finite element model with mixed elements

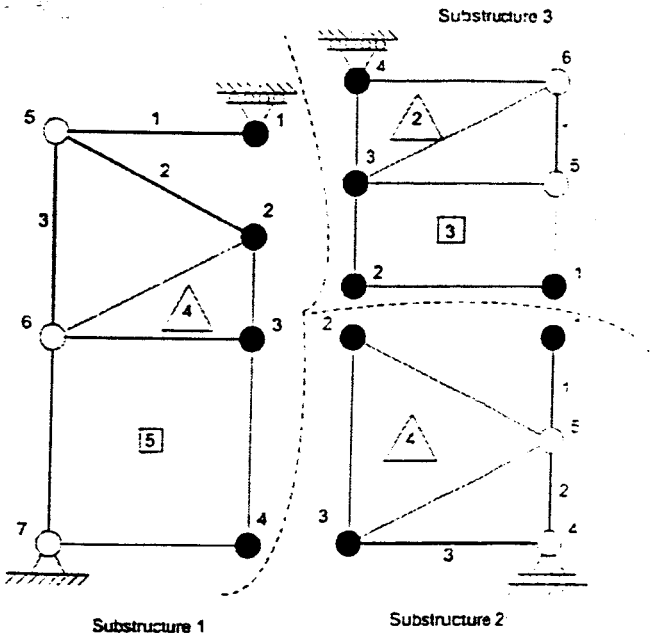

Figure 4. Decomposition of mixed model into three subdomains

final numerical results using the DIPSS software. This small-scale example was also solved in Matlab using separate software packages. Although numerical results are

not presented for the sake of brevity, excellent comparison between DIPSS and the Matlab solution was obtained for this small-scale example problem.

4.3. Example 2 – Three dimensional structural bracket finite element model. The DD formulation has also been applied to solve the 3-D structural bracket problem shown in Figure 5. The finite element model contains 194,925 degrees of freedom (N=194,925) and the elements in the matrix, K, are real. Results were computed on a cluster of 1-6 personal computers (PCs) running under the Windows environment with Intel Pentium IV processors. It should be noted that the DIPSS software was not ported to the PC cluster, but the DD formulation was programmed (from scratch, in C^{++}) on the cluster.

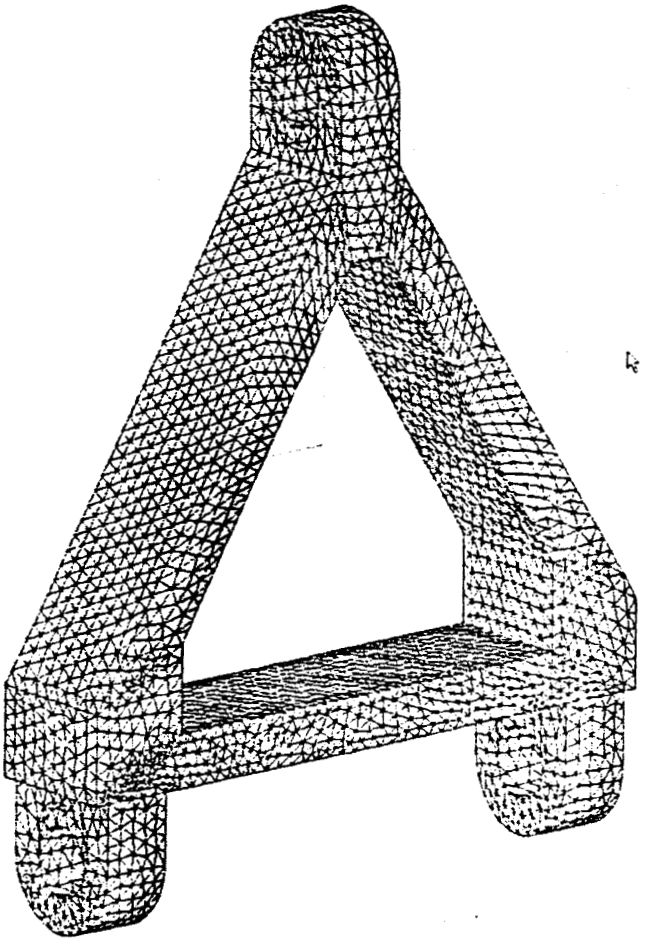

Figure 5. Finite element model for a three-dimensional structural bracket

The wallclock time (in seconds) to solve this example is documented in Table 1. A superlinear speedup factor of 10.35 has been achieved when 6 processors were used.

# of PC processors	1	2	3	4	5	6
Wallclock time (sec)	2,670	700	435	405	306	258
Speedup factor	1.00	3.81	6.14	6.59	8.73	10.35

Table 1: 3-D Structural bracket model (194.925 dofs, K real)

4.3. Example 3 – Three dimensional acoustic finite element model. In this final example, DIPSS is exercised to study the propagation of plane acoustic pressure waves in a 3-D hard wall duct without end reflection and airflow.

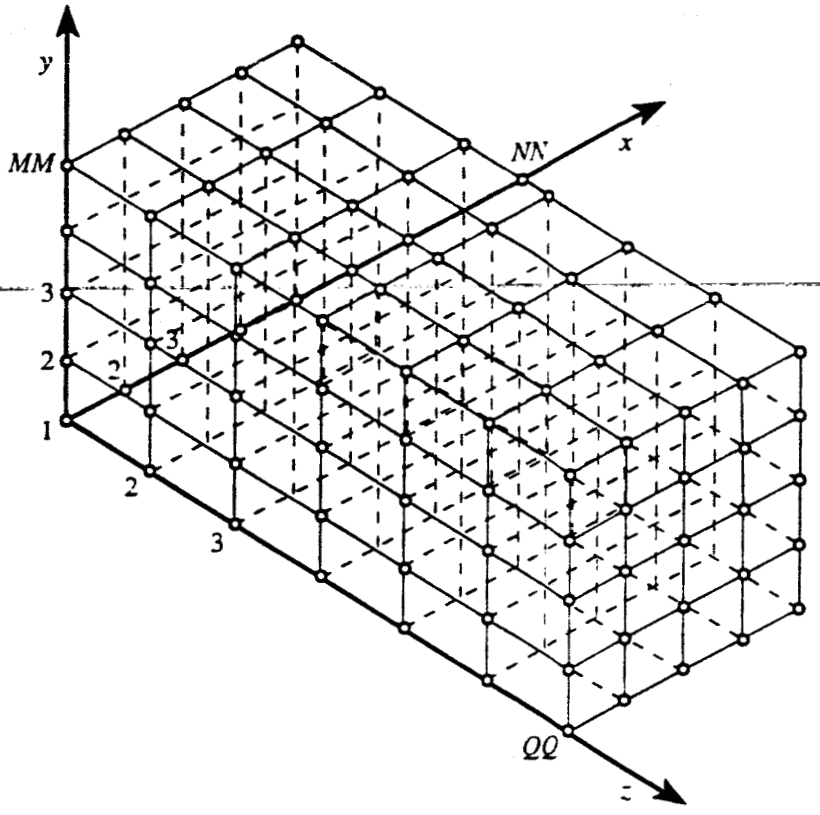

Figure 6. Finite element model for a three-dimensional hard wall duct

The duct is shown in Figure 6 and is modelled with brick elements. The source and exit planes are located at the left and right boundary, respectively. The matrix, K, contains complex coefficients and the dimension of K is determined by the product of NN, MM, and QQ (N=MMxNNxQQ). Results are presented for two

grids (N=751,513 and N=1,004,400) and the finite element analysis procedure for generation of the complex stiffness matrix, K, was presented in another paper [18].

DIPSS memory and wallclock statistics were also compared to those obtained using the platform specific SGI parallel sparse solver (i.e., ZPSLDLT). These statistics were computed on an SGI ORIGIN 2000 computer platform that was located at the NASA Langley Research Center. The SGI platform contained 10 gigabytes of memory and eight ORIGIN 2000 processors were used. It should be noted that ZPSLDLT is part of the SCSL library (version 1.4 or higher) and is considered to be one of the most efficient commercialized direct sparse solvers that is capable of performing complex arithmetic. Due to the 3-D nature of hard wall duct example problem, K encounters many fill-in elements during the factorization phase. Thus, only the small grid (N=751,513) could fit within the allocated memory on the ORIGIN 2000. ZPSLDLT required 6.5 wallclock hours to obtain the solution on the small grid whereas DIPSS wallclock was only 2.44 hours. DIPSS also required nearly 1 gigabyte less memory than ZPSLDLT, and the DIPSS and ZPSLDLT solution vector (Z) were in excellent agreement.

Because DIPSS uses MPI for interprocess communications, it can be ported to other computer platforms. To illustrate this point the DIPSS software was ported to the SUN 10000 platform at Old Dominion University and used to solve the large grid duct acoustic problem (N =1,004,400). Wallclock statistics and speedup factors were obtained using as many as 64 SUN 10000 processors. Results are presented in Table 2. It should be noted that a superlinear speedup factor of 85.95 has been achieved

# of SUN processors	1	2	4	8	16	32	64
Assembly time (sec)	19.38	10.00	5.08	2.49	1.26	0.70	0.27
Factor time (sec)	131.229	58.976	26.174	10.273	3.260	909	56
Wallclock time (sec)	131.846	61.744	27.897	11.751	3.817	1.967	1.534
Speedup factor	1.00	2.14	4.73	11.22	34.54	67.03	85.95

Table 2: Statistics for 3-D Hard wall duct (N=1,004,400, K complex)

when 64 SUN 10000 processors are used. This super-linear speedup factor is due to two primary reasons:

(1) The large finite element model has been divided into 64 subdomains. Since each processor is assigned to a smaller subdomain, the number of operations performed by each processor has been greatly reduced. Note that the number of operations are proportional to $(n^{(r)})^3$ for the dense matrix, or $n^{(r)} \cdot BW^2$ for the banded, sparse matrix, where BW represent the half Band Width of the coefficient stiffness matrix.

(2) When the entire finite element model is analyzed by a direct conventional sparse solver, more computer "paging" is required due to a larger problem size.

5. Conclusions

A domain decomposition (DD) formulation for solving sparse linear systems of equations has been presented. The formulation incorporates lower level novel algorithmic ideas such as mixed direct/iterative sparse solvers, equation reordering, loop unrolling, efficient sparse assembly, and foward/backward solution phases that are optimized to take full advantage of sparsity and exploit modern computer architecture. Medium to large-scale examples considered in this paper show that the developed MPI parallel DD code is efficient in both sequential and parallel computing environments. Statistics show that software based on the formulation is significantly more efficient than that based on one of the best available commercialized, parallel, direct sparse solver.

Acknowledgement. The authors would like to acknowledge the many helpful comments suggested by the reviewers of this paper and the NASA Langley Research Center for providing financial support.

REFERENCES

1. DESAI, CHANDRAKANT S. and ABEL, JOHN F.: *Introduction to the Finite Element Method*, Van Nostrand Reinhold Company, New York, N.Y., 1972.
2. BATHE, K. J.: *Finite Element Procedures*, Prentice-Hall, Inc., 1996.
3. NGUYEN, D.T.: *Parallel-Vector Equation Solver For Finite Element Engineering Applications*, Kluwer Academic/Plenum Publishers, 2002.
4. QIN, J., GRAY, JR., C .E., MEI, C. and NGUYEN, D. T.: *A parallel-vector equation solver for unsymmetric matrices on supercomputers*, Computing Systems in Engineering, **2**(2/3), (1991), 197-290.
5. NGUYEN, D. T., RUNESHA, H., BELEGUNDU, A. D., and CHANDRUPATLA, T. R.: *Interior point method and indefinite sparse solver for linear programming problems*, Advances in Engineering Software, **29**(3-6), (1998) 409-414.
6. NGUYEN, D.T., HOU, GENE, RUNESHA, H. and BANGFEI, H.: *Alternative approach for solving sparse indefinite symmetrical system of equations*, Advances in Engineering Software, **31**(8-9), (2000), 581-584.
7. NG, E. and PEYTON, B.: *Block sparse Choleski algorithm on advanced uniprocessor computer*, Society for Industrial and Applied Mathematics Journal of Scientific Computing, **14**, (1993), 1034-1056.
8. DUFF, I. and REID, J.: *MA27-A set of Fortran Subroutines for Solving Sparse Symmetric Sets of Linear Equations*, AERE Technical Report, R-10533. Harwell, England, 1982.
9. DUFF, I. and REID, J.: *The multifrontal solution of indefinite sparse symmetric linear systems*, Association for Computing Machinery Transactions Mathematical Software, **9**, (1983), 302-325.
10. GEORGE, A. and LIU, J.: *Computer Solution of Large Sparse Positive Definite Systems*, Prentice-Hall, Inc., Englewood Cliffs, NJ, Chap. 5 & Chap. 10. 1981.
11. PISSANETZKY, S.: *Sparse Matrix Technology*, Academic Press, Inc., London, U.K., 1984.
12. MOAYYAD, M. A. and NGUYEN, D. T.: *An algorithm for domain decomposition in finite element analysis*, Journal of Computers and Structures, **39**(1-4), (1991), 277-290.

13. KARYPIS, G. and KUMAR, V.: *METIS: Unstructured Graph Partitioning and Sparse Matrix Ordering*, Version 2.0, University of Minnesota, 1995.

14. TUNGKAHOTARA, S., NGUYEN, D. T., WATSON, W. R. and RUNESHA, H. B.: *Simple and efficient parallel dense equation solvers*, Ninth International Conference on Numerical Methods and Computational Mechanics, July 15-19, 2002, Univ. of Miskolc, Miskolc, Hungary.

15. ANDERSON, E., BAI, Z., BISCHOF, C., BLACKFORD, L. S., and DEMMEL, J. W.: *Lapack Users' Guide (Software, Environments and Tools, 9)*, Society for Industrial & Applied Mathematics; ISBN: 0898714478; 3rd pkg edition, 2000.

16. BLACKFORD, L. S., CHOI, J., CLEARY, A., D'AZEVEDO, E. and DEMMEL, J. W.: *Scalapack Users' Guide*, Society for Industrial & Applied Mathematics; ISBN: 0898713978; Bk&Cdr edition, 1997.

17. PAPADRAKAKIS, M., BITZARAKIS, S. and KOTSOPULOS, A.: *Parallel Solution Techniques in Computational Structural Mechanics*, B. H. V. Topping (Editor), Parallel and Distributed Processing for Computational Mechanics: Systems and Tools, pp. 180-206, 1999, Saxe-Coburg Publications, Edinburgh. Scotland.

18. WATSON, W. R.: *Three-dimensional rectangular duct code with application to impedance eduction*, AIAA Journal, 40, (2002), 217-226.

4. Parallel Finite Element Domain Decomposition [Refs. 6.6, 6.8] for Structural/Acoustic Analysis: Un_symmetrical Case

The finite elelement DD formulation for the "unsymmetrical" matrix case is essentially the same as the "symmetrical" case, discussed in Section 3 of this report. Following are the major differences between these 2 cases:

(a) Re-ordering algorithms (to minimize fill-in terms), sparse assembly strategies, and sparse solvers used in the "symmetrical" case need to be modified for the "unsymmetrical" case.

(b) The Pre_conditioned Conjugate Gradient (PCG) iterative solver for solving the boundary displacement vector (for "symmetrical" case) needs to be replaced by the Pre_conditioned Bi-Conjugate Gradient (with stabilized schemes) [Ref. 6.7] for "unsymmetrical" case.

For "multiple" processors computation, mixed iterative (BiCG

with Stabilized strategies) and direct sparse, unsymmetrical

solvers are used. However, the BiCG unsymmetrical iterative

solver seems to be "NOT robust" enough to solve the unsymmetrical

finite element acoustic problems. Thus, further investigation on

this topic is needed !

However, for a "single processor" (or serial computation) execution, since only the sparse, unsymmetrical "direct" solver is used, the obtained finite element accoustic results seem to be robust, and reliable.

The Makefile, all source codes (including all .f, and all .c files), input data file (= fort.501, with explanation), output data file (= fort.700) etc... can be obtained from the PI's (Prof. Nguyen's) ODU SUN account, at:

cd ~/cee/dd_unsym_fem_complex_acoustic_willie/

Notice that the main program is stored under file name "cddmain.f".

5. Summary of Accomplishments and Deliverable Items

Years 1 and 2 (January 2001 - January 2003)

(a) A first journal paper (on sparse assembly & solver) has been published [Ref. 6.1]

(b) NASA LaRC Finite Element [Ref. 6.12] acoustic assembly time has been significantly reduced [refer to Table 1 of Section 2]

(c) Symmetrical sparse re-ordering algorithms/sofware, such as Multiple Minimum Degree (MMD), Nested Disection (ND) [Ref. 6.4] have been incorporated into the finite element procedures.

(d) Symmetrical sparse symbolic & numerical "assembly" software have been integrated into the finite element procedures.

(e) Symmetrical sparse symbolic & numerical "factorization" software, including unrolling strategies [Ref. 6.5, Chapter 10] have been developed and integrated into the finite element procedures.

(f) Symmetrical sparse "forward and backward solution" software, including unrolling strategies [Ref. 6.5, Chapter 10] have been developed and integrated into the finite element procedures.

(g) A second journal paper (on Parallel FE, DD formulation) has been published [Ref. 6.2]

(h) Parallel DD Pre_conditioned Conjugate Gradient (PCG) iterative solver (for symmetrical matrix case) software has been developed.

REMARKS:

METiS [Ref. 6.3] (a software which has the capabilities to minimize fill-in terms during the sparse factorization phase, and to automatically split a large finite element model into smaller sub-domains) has NOT yet been incorporated into the developed DD FE code. Instead, "hard coded" domain splitting has been used.

Years 3 and 4 (January 2003 - January 2005)

(i) Un_symmetrical sparse symbolic & numerical "assembly" software have been integrated into the finite element procedures.

(j) Un_symmetrical sparse symbolic & numerical "factorization" software, including unrolling strategies [Ref. 6.5, Chapter 10] have been developed and integrated into the finite element procedures.

(k) Un_symmetrical sparse "forward and backward solution" software, including unrolling strategies have been developed and integrated into the finite element procedures.

(l) METiS [Ref. 6.3] (a software which has the capabilities to minimize fill-in terms during the sparse factorization phase, and to automatically split a large finite element model into smaller sub-domains) has recently been incorporated into the developed DD FE code.

(m) Parallel DD [Ref. 6.6] Pre_conditioned Bi_CG iterative solver [Ref. 6.7] (for un_symmetrical matrix case) software has been developed.

However, the Bi_CG iterative solver (with DD formulation) and its communication strategies (amongst different processors) need further studies to improve the robustness of the algorithms !

REMARKS:

"Extra" works to investigate the possibilities of using the software MA28 [see Ref. 6.10], seperating the factorized and forward/backward phases in the sparse solver package SUPER-LU [see Ref. 6.9] etc... have also been conducted by Dr. Nguyen's (PI's) research team at Old Dominon University (ODU) during the grant periods.

6. References

[6.1] W.R. Watson, D.T. Nguyen. C.J. Reddy, V.N. Vatsa, and W.H. Tang, "Algorithms and Application of Sparse Matrix Assembly and Equation Solvers for Aeroacoustics", AIAA Journal, Volume 40, No. 4, pages 661-670 (April'2002)

[6.2] D.T. Nguyen, W.R. Watson. S. Tungkahotara, and S.D. Rajan, "Parallel Finite Element Domain Decomposition for Structural/Acoustic Analysis", Journal of Computational and Applied Mechanics, Vol. 4, No. 2, pages 189-201 (2003).

[6.3] Karypis, G., and Kumar, V.. "ParMETiS: Parallel Graph Patitioning and Sparse Matrix Ordering Library", University of Minnesota, Department of Computer Science, Version 2.0, 1998.

[6.4] George, J.A., and Liu, W.H.. Computer Solution of Large Sparse Positive Definite Systems, Prentice-Hall, Englewood Cliffs, NJ (1981)

[6.5] Nguyen,Duc T.,"Parallel-Vector Equation Solvers for Finite Element Engr. Applications", by Kluwer/Plenum Academics Publisher (2002)

[6.6] Nguyen,Duc T., "Finite Element Methods: Parallel-Sparse Statics and Eigen-Solutions", Graduate level textbook, Expected date of completion: April 28, 2005

[6.7] R. Barrett, M. Berry, T. Chan, J. Demmel, J. Donato, J. Dongara, V. Eighout, R. Pozo, C. Romine, and H.V. der Vorst, "Templates for the Solution of Linear Systems: Building Blocks for Iterative Methods", SIAM, 1994

[6.8] Arora, J.S. and Nguyen, D.T., "Eigen-solution for Large Structural Systems with Substructures", International Journal for Numerical Methods in Engineering, Vol. 15, 1980, pp. 333-341.

[6.9] J.W. Demmel, J.R. Gilbert, and X.S. Li, "SuperLU Users' Guide", September 21, 1999

[6.10] I.S. Duff, "MA28-a set of FORTRAN subroutines for solving sparse unsymmetric sets of linear equations". Technical Report R.8730, AERE, Harwell, England, 1982

[6.11] SGI (library subroutines) sparse solver

[6.12] W.R. Watson, "Three-Dimensional Rectangular Duct Code With Application to Impedance Eduction", AIAA Journal, 40, pp. 217-226 (2002)

7. Acknowledgements

The PI (Duc T. Nguyen) would like to express his appreciation for the financial supports, provided by the NASA Langley Research Center, of this project. Dr. Willie Watson (at NASA LaRC), not only served a super job as a Technical Monitor, but he has also actively involved in the contributions of some of his "finite element acoustic subroutines", and providing many useful inputs, discussions during the verification phase of the developed codes.

The PI also expresses his appreciation for the contributions from several members of his ODU research team, such as Mr. Tungkahotara (Ph.D student), Dr. J. Qin (former Post-Doctoral Research Associate), and Dr. H. Runesha (former Ph.D student).

Finally, the computer facilities provided by NASA Langley Research Center, and Old Dominion University (OCCS) are also greatfully acknowledged.